Amplitude analysis methods

Anton Poluektov

The University of Warwick, UK
Budker Institute of Nuclear Physics, Novosibirsk, Russia

27 September 2016

Introduction

Amplitude analyses play more and more important role at LHCb as we gain experience

- Require good understanding of the detector and background, tools and computing resources.
- More powerful than counting techniques: access to quantum numbers, control of reflections and phase-space effects, model-independent approaches

Various techniques with illustrations from published analyses

- Traditional Dalitz plot analyses
  - Helicity, Zemach, covariant formalisms for angular terms
  - Isobar model, K-matrix for lineshapes
- (Semi) model-independent approaches
  - Legendre moments: study of partial wave composition, need for exotic contributions
  - Splines or bins in m^2: confirmation of resonant phase rotation
- Amplitude analyses of 3-body decays with non-scalars in final state
- Amplitude analyses of baryonic decays

Amplitude analyses at LHCb

The ones I will mention. Certainly not a complete list.

Analysis	Contributions	Approaches
$B^0 \to \overline{D}^0\pi^+\pi^-$	$D^{**-} \to \overline{D}^0\pi^-$; $\pi^+\pi^-$	Dalitz; Isobar; K-matrix
$B_s^0 \to \overline{D}^0 K^-\pi^+$	$D_s^* \to \overline{D}^0 K^-$; $K^* \to K^-\pi^+$	Dalitz; Isobar
$B^0 \to \overline{D}^0 K^+\pi^-$	$D^{*-} \to \overline{D}^0\pi^-$; $K^* \to K^-\pi^+$	Dalitz; Isobar
$B^- \to D^+K^-\pi^-$	$D^{**0} \to D^-\pi^+$	Dalitz; Isobar; Legendre
$B^- \to D^+\pi^-\pi^-$	$D^{**0} \to D^-\pi^+$	Dalitz; Isobar; Legendre; Splines
$B^0 \to \psi'\pi^-K^+$	$K^* \to K^-\pi^+$; $\psi'\pi^-$	Non-scalar; Isobar; Bins; Legendre
$B^+ \to J/\psi\,\phi K^+$	$K^* \to \phi K^+$; $J/\psi\,\phi$	Non-scalar; Isobar;
$\Lambda_b^0 \to J/\psi\,pK^-$	$\Lambda^* \to pK^-$; $J/\psi\,p$	Baryon; Isobar; Bins; Legendre
$\Lambda_b^0 \to J/\psi\,p\pi^-$	$N^* \to p\pi^-$; $J/\psi\,p + J/\psi\,\pi^-$?	Baryon; Isobar; K-matrix

Dalitz plot analyses

- Two-body decays $D \to ab$: kinematics is completely fixed by conservation laws: no access to the amplitude
- Three-body decays $D \to abc$ (all scalars): after taking into account trivial rotations, two internal degrees of freedom remain. Can take any pair of independent parameters as variables for amplitude parametrization: **Dalitz plot**.

Phase space is uniform in variables m^2_{ab}, m^2_{bc}:

$$d\Gamma = \frac{1}{(2\pi)^3}\frac{1}{32M^3}|\mathcal{A}(m^2_{ab}, m^2_{bc})|^2 dm^2_{ab} dm^2_{bc}\,.$$

Any non-uniformity is due to dynamical properties of amplitude $\mathcal{A}(m^2_{ab}, m^2_{bc})$.

Isobar model: sum of line shapes with angular terms

$$\mathcal{A} = \sum_i A_i \times R^{(i)}(m^2_1) \times T^{(i)}_J(m^2_2)$$

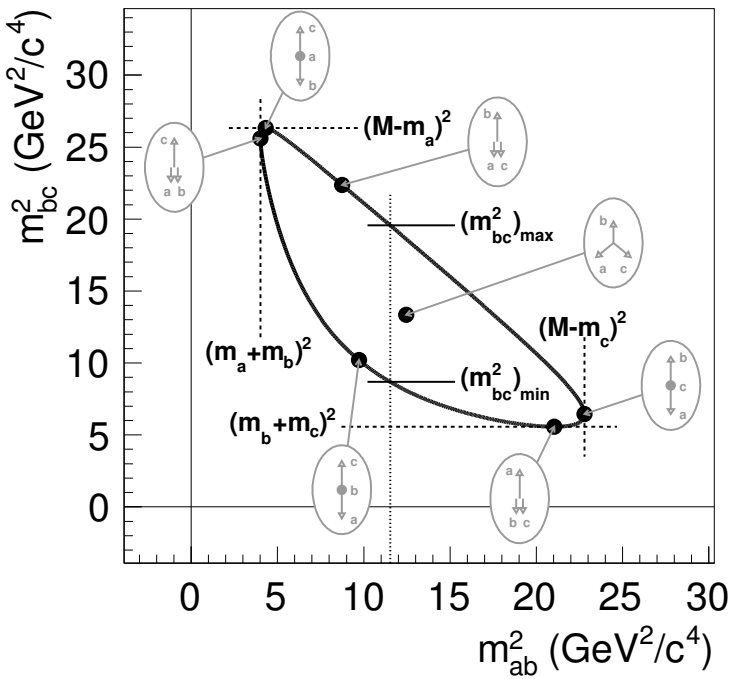

Dalitz plot analyses

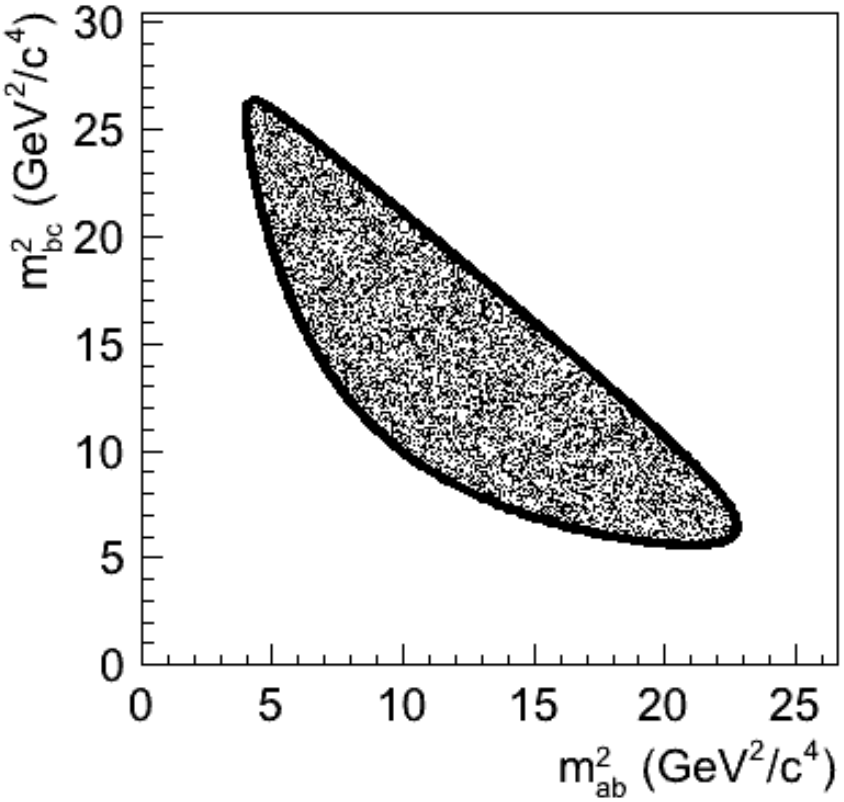

- Phase-space decay
- Scalar in *bc* channel
- Scalar in *ac* channel
- Scalar in *ab* channel
- Vector in *ab* channel
- Tensor ($J = 2$) in *ab* channel
- Two scalars in *ab* and *bc* channels, $\Delta\phi = 0^\circ$
- Two scalars in *ab* and *bc* channels, $\Delta\phi = 90^\circ$
- Two scalars in *ab* and *bc* channels, $\Delta\phi = 180^\circ$
- Scalar and vector in *ab* channel, $\Delta\phi = 0^\circ$

Dalitz plot analyses

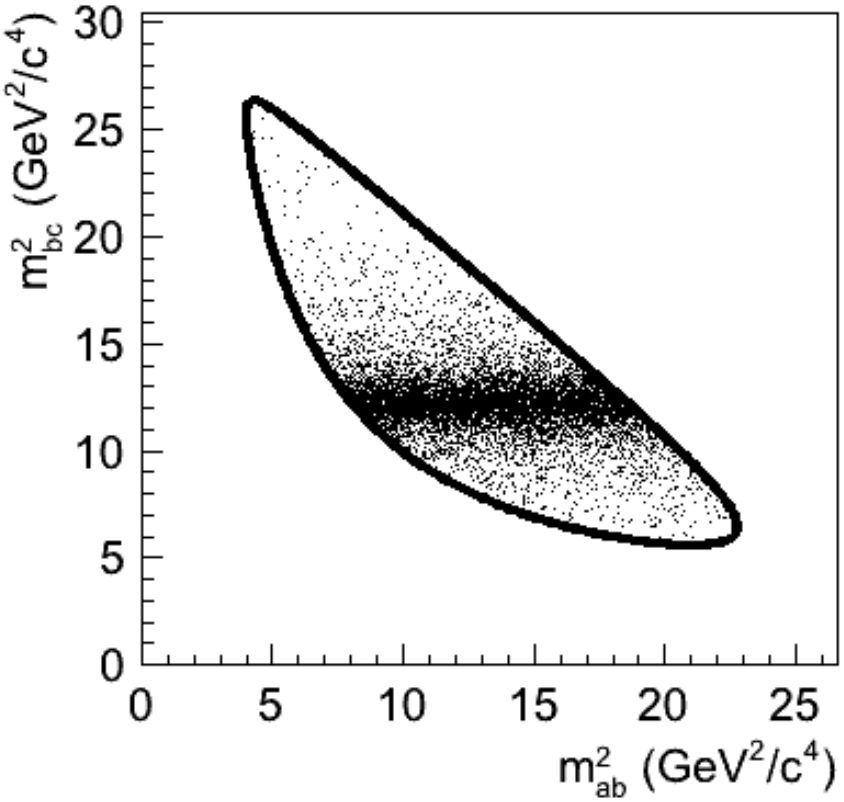

- Phase-space decay
- Scalar in *bc* channel
- Scalar in *ac* channel
- Scalar in *ab* channel
- Vector in *ab* channel
- Tensor ($J = 2$) in *ab* channel
- Two scalars in *ab* and *bc* channels, $\Delta\phi = 0^\circ$
- Two scalars in *ab* and *bc* channels, $\Delta\phi = 90^\circ$
- Two scalars in *ab* and *bc* channels, $\Delta\phi = 180^\circ$
- Scalar and vector in *ab* channel, $\Delta\phi = 0^\circ$

Dalitz plot analyses

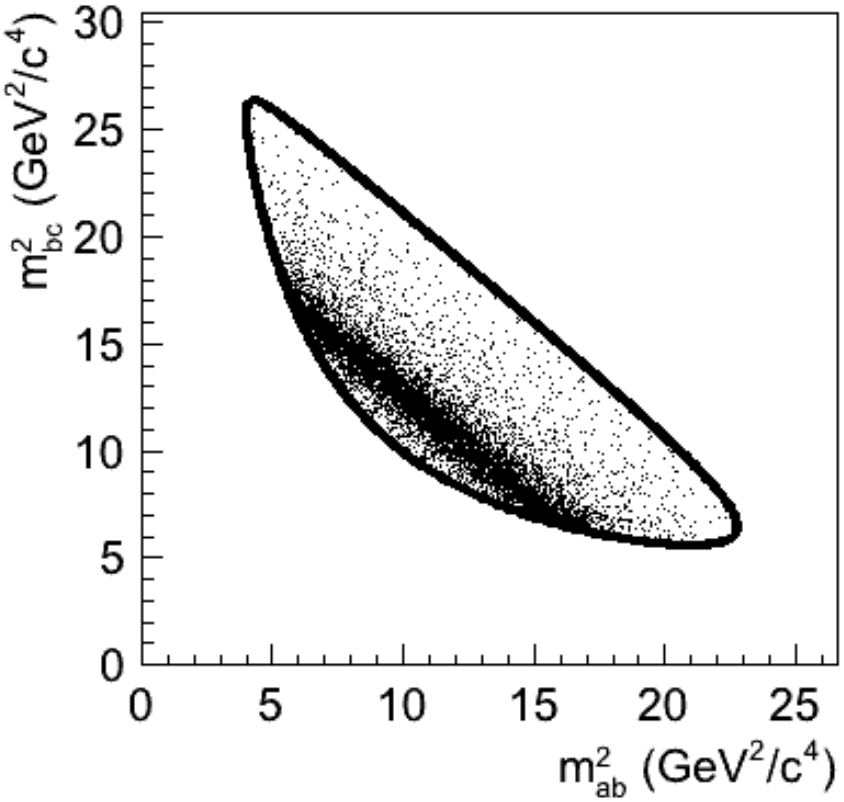

- Phase-space decay
- Scalar in *bc* channel
- Scalar in *ac* channel
- Scalar in *ab* channel
- Vector in *ab* channel
- Tensor ($J = 2$) in *ab* channel
- Two scalars in *ab* and *bc* channels, $\Delta\phi = 0^\circ$
- Two scalars in *ab* and *bc* channels, $\Delta\phi = 90^\circ$
- Two scalars in *ab* and *bc* channels, $\Delta\phi = 180^\circ$
- Scalar and vector in *ab* channel, $\Delta\phi = 0^\circ$

Dalitz plot analyses

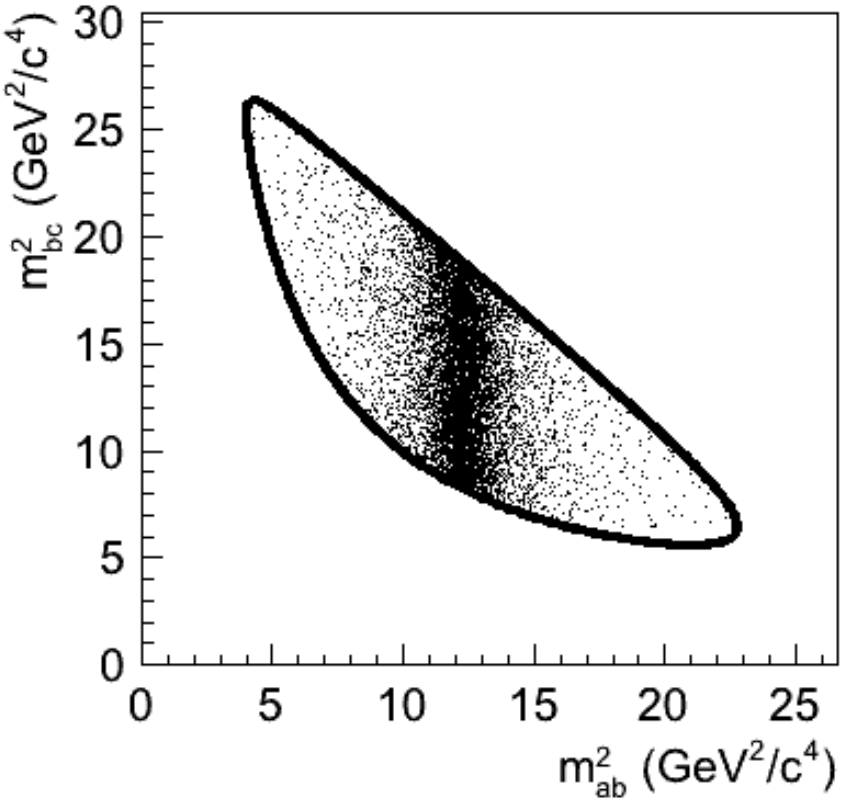

- Phase-space decay
- Scalar in *bc* channel
- Scalar in *ac* channel
- Scalar in *ab* channel
- Vector in *ab* channel
- Tensor ($J = 2$) in *ab* channel
- Two scalars in *ab* and *bc* channels, $\Delta\phi = 0^\circ$
- Two scalars in *ab* and *bc* channels, $\Delta\phi = 90^\circ$
- Two scalars in *ab* and *bc* channels, $\Delta\phi = 180^\circ$
- Scalar and vector in *ab* channel, $\Delta\phi = 0^\circ$

Dalitz plot analyses

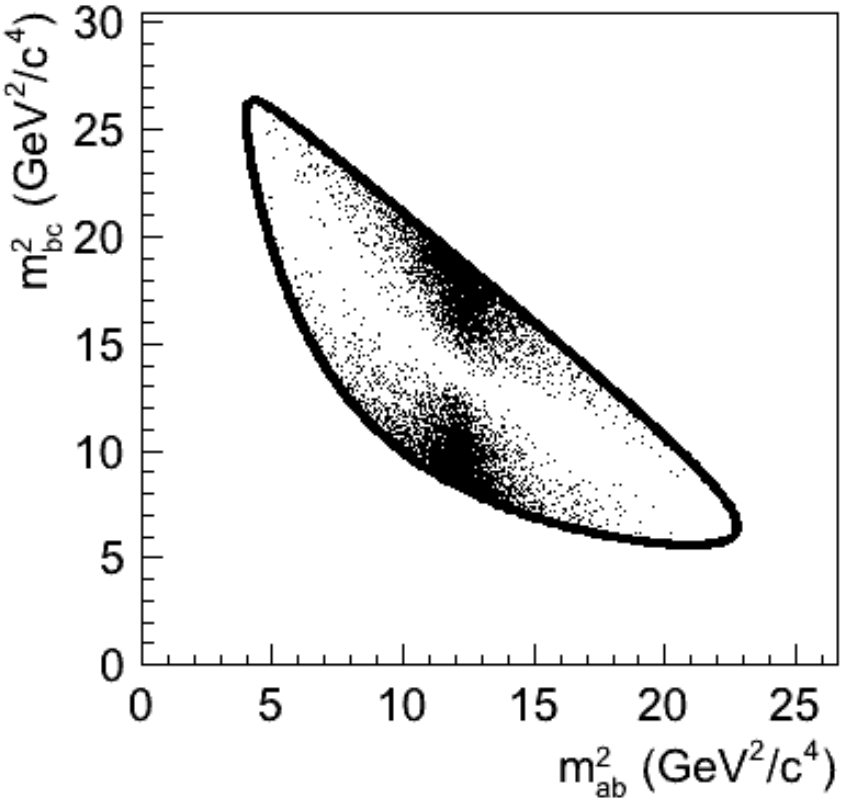

- Phase-space decay
- Scalar in *bc* channel
- Scalar in *ac* channel
- Scalar in *ab* channel
- Vector in *ab* channel
- Tensor ($J = 2$) in *ab* channel
- Two scalars in *ab* and *bc* channels, $\Delta\phi = 0^\circ$
- Two scalars in *ab* and *bc* channels, $\Delta\phi = 90^\circ$
- Two scalars in *ab* and *bc* channels, $\Delta\phi = 180^\circ$
- Scalar and vector in *ab* channel, $\Delta\phi = 0^\circ$

Dalitz plot analyses

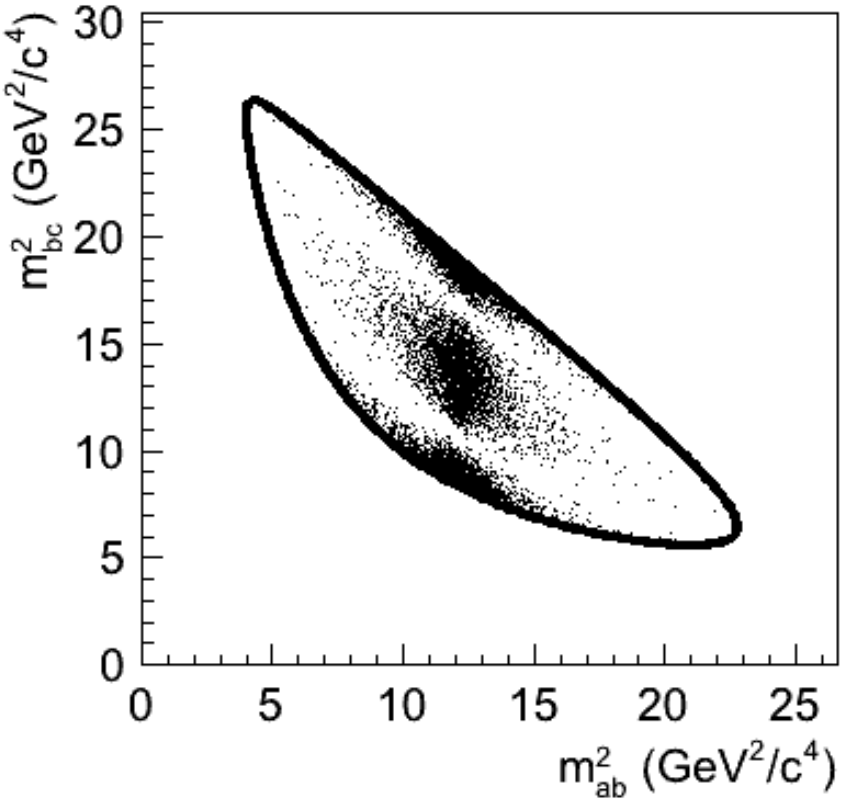

- Phase-space decay
- Scalar in *bc* channel
- Scalar in *ac* channel
- Scalar in *ab* channel
- Vector in *ab* channel
- Tensor ($J = 2$) in *ab* channel
- Two scalars in *ab* and *bc* channels, $\Delta\phi = 0^\circ$
- Two scalars in *ab* and *bc* channels, $\Delta\phi = 90^\circ$
- Two scalars in *ab* and *bc* channels, $\Delta\phi = 180^\circ$
- Scalar and vector in *ab* channel, $\Delta\phi = 0^\circ$

Dalitz plot analyses

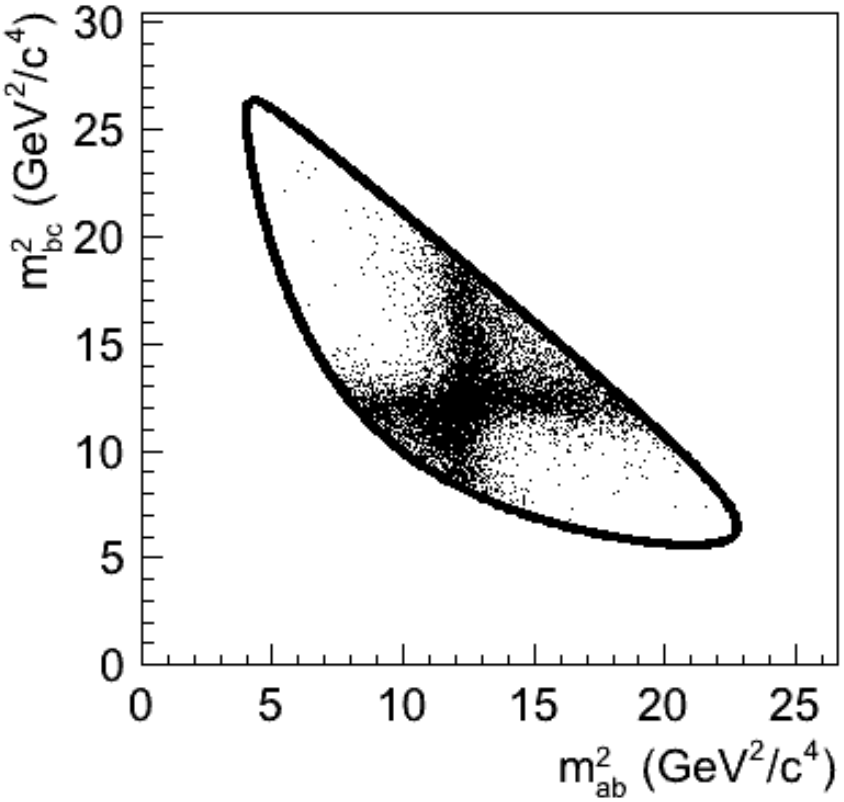

- Phase-space decay
- Scalar in *bc* channel
- Scalar in *ac* channel
- Scalar in *ab* channel
- Vector in *ab* channel
- Tensor ($J = 2$) in *ab* channel
- Two scalars in *ab* and *bc* channels, $\Delta\phi = 0^\circ$
- Two scalars in *ab* and *bc* channels, $\Delta\phi = 90^\circ$
- Two scalars in *ab* and *bc* channels, $\Delta\phi = 180^\circ$
- Scalar and vector in *ab* channel, $\Delta\phi = 0^\circ$

Dalitz plot analyses

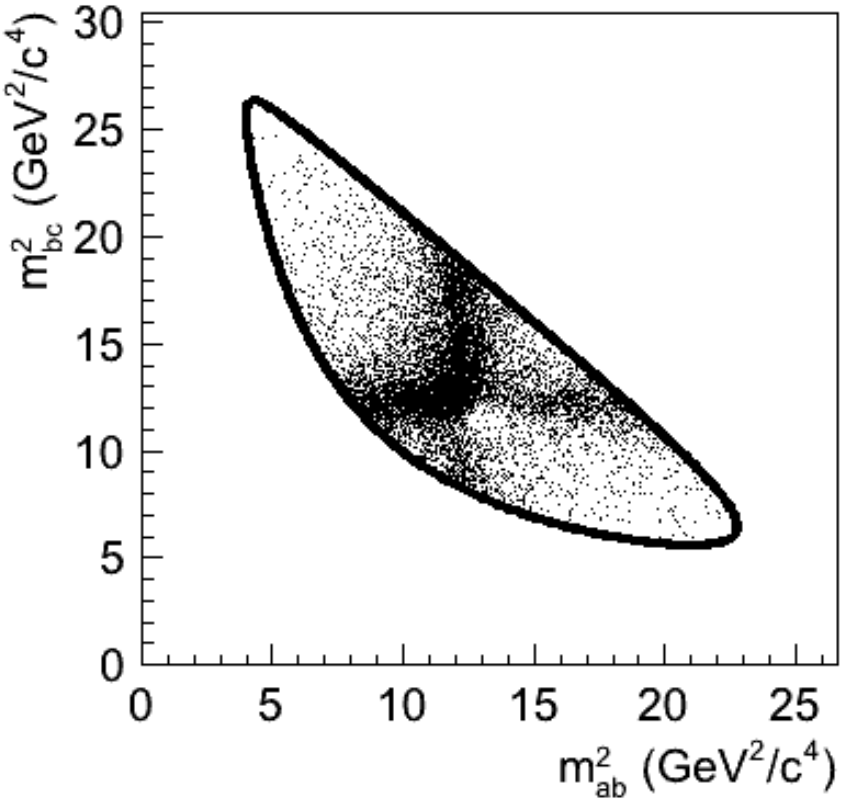

- Phase-space decay
- Scalar in *bc* channel
- Scalar in *ac* channel
- Scalar in *ab* channel
- Vector in *ab* channel
- Tensor ($J = 2$) in *ab* channel
- Two scalars in *ab* and *bc* channels, $\Delta\phi = 0^\circ$
- Two scalars in *ab* and *bc* channels, $\Delta\phi = 90^\circ$
- Two scalars in *ab* and *bc* channels, $\Delta\phi = 180^\circ$
- Scalar and vector in *ab* channel, $\Delta\phi = 0^\circ$

Dalitz plot analyses

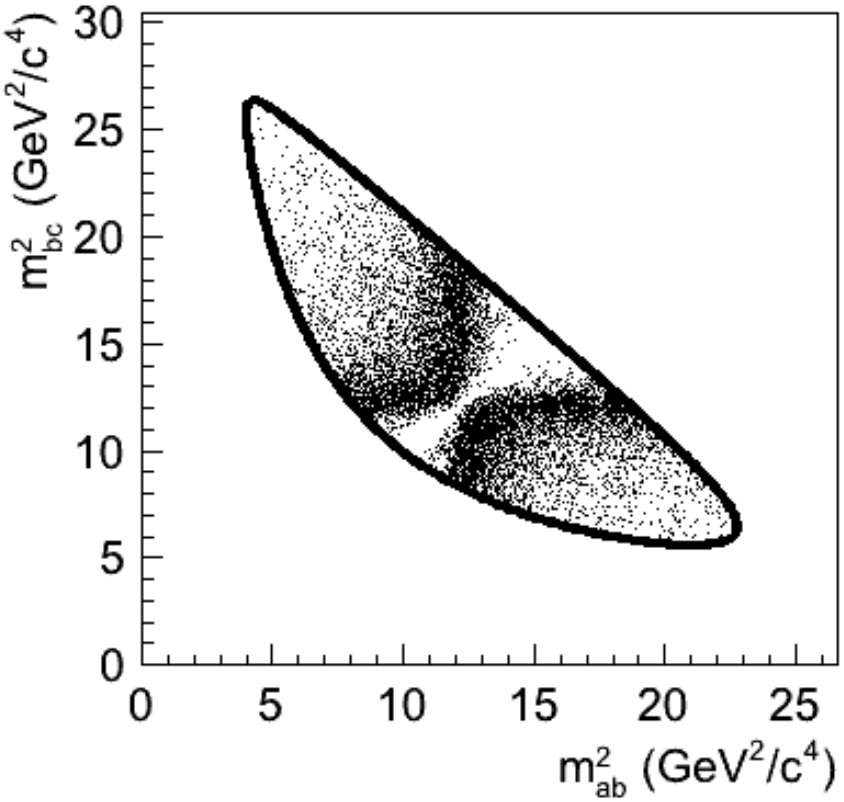

- Phase-space decay
- Scalar in *bc* channel
- Scalar in *ac* channel
- Scalar in *ab* channel
- Vector in *ab* channel
- Tensor ($J = 2$) in *ab* channel
- Two scalars in *ab* and *bc* channels, $\Delta\phi = 0^\circ$
- Two scalars in *ab* and *bc* channels, $\Delta\phi = 90^\circ$
- Two scalars in *ab* and *bc* channels, $\Delta\phi = 180^\circ$
- Scalar and vector in *ab* channel, $\Delta\phi = 0^\circ$

Dalitz plot analyses

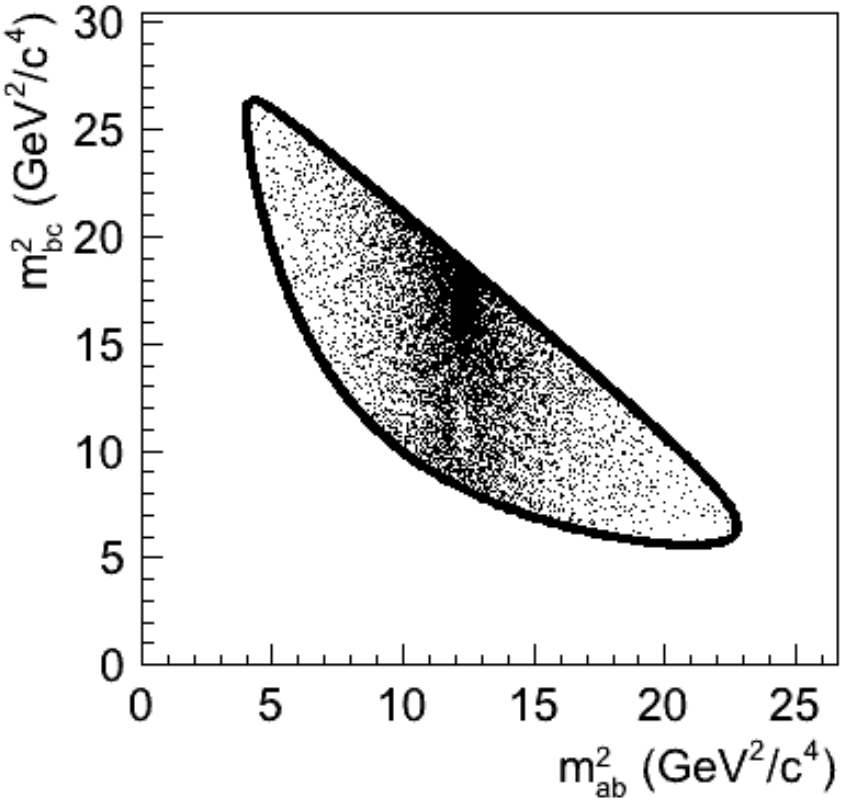

- Phase-space decay
- Scalar in *bc* channel
- Scalar in *ac* channel
- Scalar in *ab* channel
- Vector in *ab* channel
- Tensor ($J = 2$) in *ab* channel
- Two scalars in *ab* and *bc* channels, $\Delta\phi = 0^\circ$
- Two scalars in *ab* and *bc* channels, $\Delta\phi = 90^\circ$
- Two scalars in *ab* and *bc* channels, $\Delta\phi = 180^\circ$
- Scalar and vector in *ab* channel, $\Delta\phi = 0^\circ$

Dalitz plot analyses: angular terms

Helicity formalism: angular distribution as a function of helicity angle $\theta(m_{bc})$

$$M_1 = \cos\theta$$

$$M_2 = \cos^2\theta - \frac{1}{3}$$

Zemach tensors: expressions involving 3-momenta

$$M_1 = -2\vec{p}\cdot\vec{q}$$

$$M_2 = \frac{4}{3}[3(\vec{p}\cdot\vec{q})^2 - (|\vec{p}||\vec{q}|)^2]$$

Covariant formalism: covariant amplitudes expressed via projection operators

$$M_1 = (p_D + p_A)^\mu \cdot P^{(1)}_{\mu\nu}(p_A + p_B)\cdot(p_A - p_B)^\nu$$

$$M_2 = (p_D + p_A)^{\mu_1}(p_D + p_A)^{\mu_2}\cdot P^{(2)}_{\mu_1\mu_2\nu_1\nu_2}(p_A + p_B)\cdot(p_A - p_B)^{\nu_1}(p_A - p_B)^{\nu_2}$$

The three formalisms lead to the same angular distributions $T_J(m^2_{bc})$.

Not fully equivalent: modify lineshapes $R(m^2_{ab})$.

- Centrifugal term q^L: should be artificially included in $R(m^2_{ab})$ for helicity formalism
- Covariant formalism: relativistic correction in the transformation between D and R rest frames.

Dalitz plot analyses: line shapes

Breit-Wigner resonant shape with various corrections

$$R(m_{ab}^2) = \frac{B_r(\vec{q})B_D(\vec{p})}{(m_0^2 - m_{ab}^2) - im_0\Gamma(m)}$$

Mass-dependent width $\Gamma(m)$, Blatt-Weisskopf barrier factors B_i.

Flatté: if 2nd channels opens near the resonance mass

$$R(m_{ab}^2) = \frac{1}{m_0^2 - m_{ab}^2 - im_0(g_1\rho_1(m_{ab}^2) + g_2\rho_2(m_{ab}^2))}$$

"Non-resonant" shapes

$$R(m_{ab}^2) = \exp(-\alpha m_{ab}^2)$$

or more sophisticated ones (LASS, kappa, "dabba" etc.)

K-Matrix: ensure unitarity by construction (used for spin-0 $\pi^+\pi^-$ and spin-1/2 $p\pi^-$ amplitudes)

$$A_i = (I - iK\rho)_{ij}^{-1} P_j$$

Parameters of K-matrix (pole couplings and scattering amplitudes) are taken from the global analysis of $\pi^+\pi^-$ ($p\pi^-$) data.

Dalitz plot analyses: some technical details

Many of LHCb analyses use `Laura++` Dalitz plot framework (Warwick): http://laura.hepforge.org.

- Implements both model-dependent (isobar, K-matrix) and semi-model independent (splines) approaches.
- Allows to perform 2D Dalitz plot fits using unbinned likelihood.
- Implements some clever optimisations (such as caching of amplitude integrals).
- Combined likelihoods, simultaneous fits, CP violation, time-dependent fits, toy MC, etc.

Several competing packages:

- `Mint`: can do 4-body final states,
- `GooFit`: GPU calculations: used in charm analyses,

as well as private analysis-specific code.

Dalitz plot analyses: some technical details

Two approaches to handle **background**:

- **cFit**: Needs explicit background parametrisation
  - Could be difficult for multidimensional fits
  - Additional systematic due to parametrisation
- **sFit**: Statistical subtraction of the background from the sideband distribution using sWeight technique
  - Assumes no correlation between the fitted distribution and the weighting distribution (inv. mass of the mother particle)
  - Larger stat. uncertainty in case of high background

Similarly, **efficiency** can be handled by

- Explicit functional form (polynomials, kernel density, smoothed histogram *etc*)
- By including the scattered data from simulation directly into the likelihood normalisation term

Some analyses try both approaches as a cross-check (such as pentaquark in $\Lambda_b^0 \to J/\psi\, pK^-$)

Dalitz plot anlayses: $B_s^0 \to D^0 K^- \pi^+$ [PRD 90 (2014) 072003]

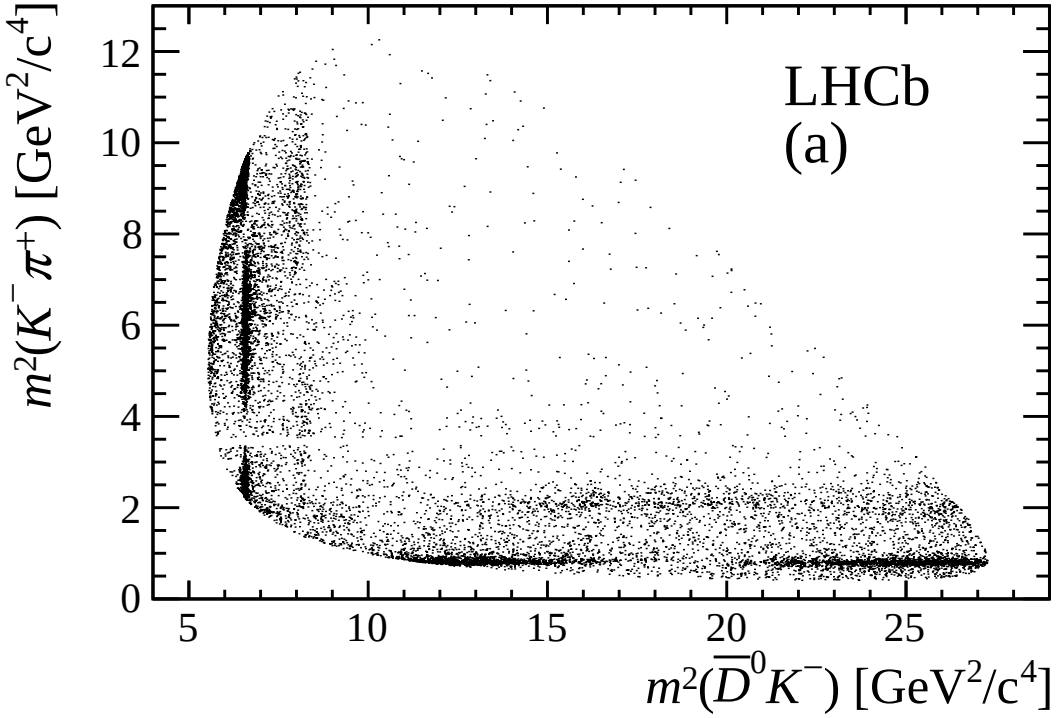

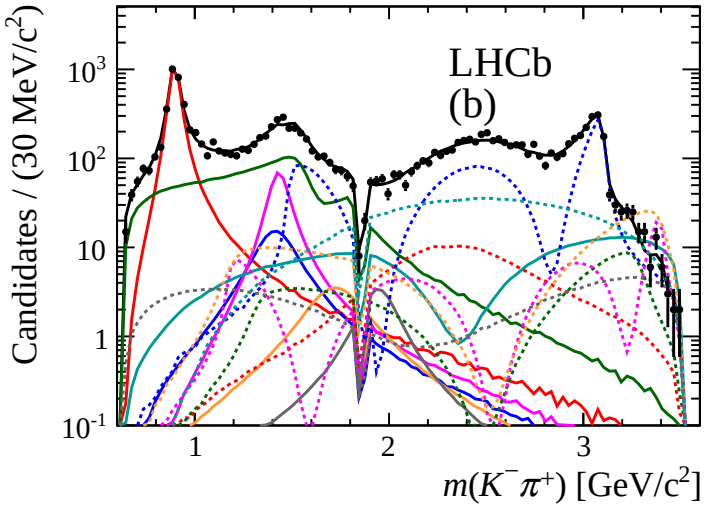

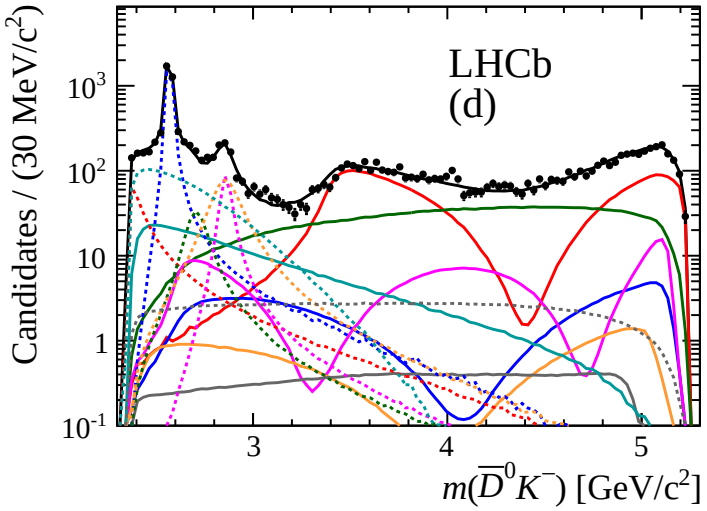

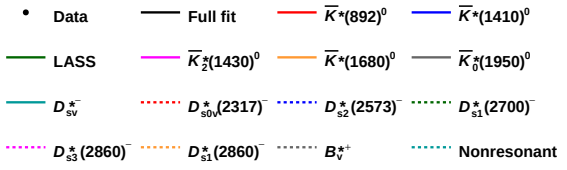

Resonance	Spin	Dalitz plot axis	Model	Parameters (MeV/c^2)
$\overline{K}^*(892)^0$	1	$m^2(K^-\pi^+)$	RBW	$m_0 = 895.81 \pm 0.19$, $\Gamma_0 = 47.4 \pm 0.6$
$\overline{K}^*(1410)^0$	1	$m^2(K^-\pi^+)$	RBW	$m_0 = 1414 \pm 15$, $\Gamma_0 = 232 \pm 21$
$\overline{K}^*_0(1430)^0$	0	$m^2(K^-\pi^+)$	LASS	See text
$\overline{K}^*_2(1430)^0$	2	$m^2(K^-\pi^+)$	RBW	$m_0 = 1432.4 \pm 1.3$, $\Gamma_0 = 109 \pm 5$
$\overline{K}^*(1680)^0$	1	$m^2(K^-\pi^+)$	RBW	$m_0 = 1717 \pm 27$, $\Gamma_0 = 322 \pm 110$
$\overline{K}^*_0(1950)^0$	0	$m^2(K^-\pi^+)$	RBW	$m_0 = 1945 \pm 22$, $\Gamma_0 = 201 \pm 90$
$D^*_{s2}(2573)^-$	2	$m^2(\overline{D}^0K^-)$	RBW	See text
$D^*_{s1}(2700)^-$	1	$m^2(\overline{D}^0K^-)$	RBW	$m_0 = 2709 \pm 4$, $\Gamma_0 = 117 \pm 13$
$D^*_{sJ}(2860)^-$	1	$m^2(\overline{D}^0K^-)$	RBW	See text
$D^*_{sJ}(2860)^-$	3	$m^2(\overline{D}^0K^-)$	RBW	See text
Nonresonant		$m^2(\overline{D}^0K^-)$	EFF	See text
$D^{*-}_{s\,v}$	1	$m^2(\overline{D}^0K^-)$	RBW	$m_0 = 2112.3 \pm 0.5$, $\Gamma_0 = 1.9$
$D^*_{s0\,v}(2317)^-$	0	$m^2(\overline{D}^0K^-)$	RBW	$m_0 = 2317.8 \pm 0.6$, $\Gamma_0 = 3.8$
B^{*+}_v	1	$m^2(\overline{D}^0\pi^+)$	RBW	$m_0 = 5325.2 \pm 0.4$, $\Gamma_0 = 0$

Dalitz plot anlayses: $B_s^0 \to D^0 K^- \pi^+$ [PRD 90 (2014) 072003]

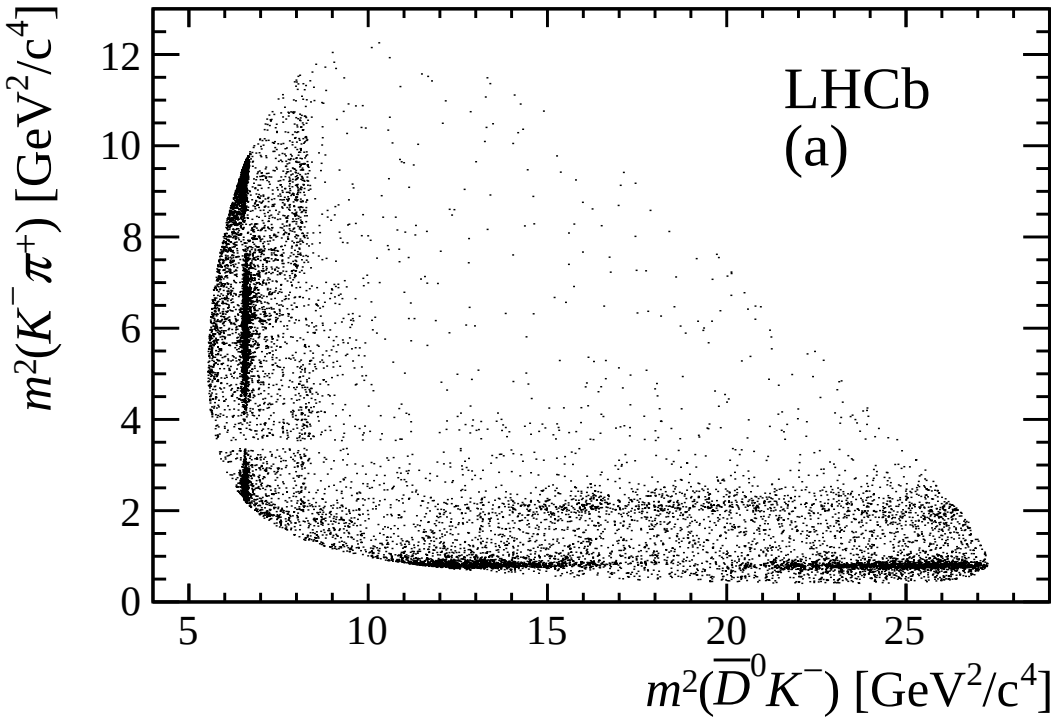

$D_{s2}(2573)$:

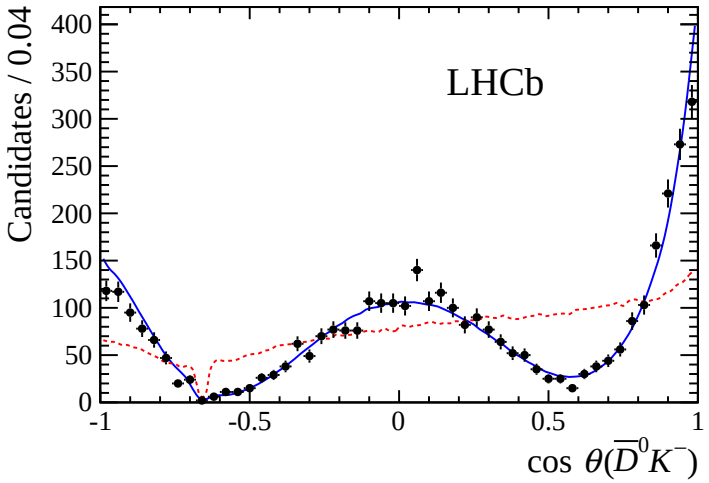

$D_{sJ}(2860)$:

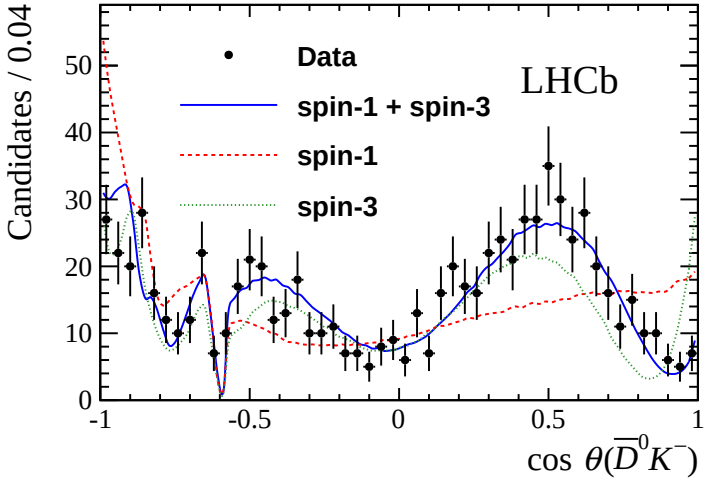

Resonance	Spin	Dalitz plot axis	Model	Parameters (MeV/c^2)
$\overline{K}^*(892)^0$	1	$m^2(K^-\pi^+)$	RBW	$m_0 = 895.81 \pm 0.19$, $\Gamma_0 = 47.4 \pm 0.6$
$\overline{K}^*(1410)^0$	1	$m^2(K^-\pi^+)$	RBW	$m_0 = 1414 \pm 15$, $\Gamma_0 = 232 \pm 21$
$\overline{K}_0^*(1430)^0$	0	$m^2(K^-\pi^+)$	LASS	See text
$\overline{K}_2^*(1430)^0$	2	$m^2(K^-\pi^+)$	RBW	$m_0 = 1432.4 \pm 1.3$, $\Gamma_0 = 109 \pm 5$
$\overline{K}^*(1680)^0$	1	$m^2(K^-\pi^+)$	RBW	$m_0 = 1717 \pm 27$, $\Gamma_0 = 322 \pm 110$
$\overline{K}_0^*(1950)^0$	0	$m^2(K^-\pi^+)$	RBW	$m_0 = 1945 \pm 22$, $\Gamma_0 = 201 \pm 90$
$D_{s2}^*(2573)^-$	2	$m^2(\overline{D}^0K^-)$	RBW	See text
$D_{s1}^*(2700)^-$	1	$m^2(\overline{D}^0K^-)$	RBW	$m_0 = 2709 \pm 4$, $\Gamma_0 = 117 \pm 13$
$D_{sJ}^*(2860)^-$	1	$m^2(\overline{D}^0K^-)$	RBW	See text
$D_{sJ}^*(2860)^-$	3	$m^2(\overline{D}^0K^-)$	RBW	See text
Nonresonant		$m^2(\overline{D}^0K^-)$	EFF	See text
$D_{s\,v}^{*-}$	1	$m^2(\overline{D}^0K^-)$	RBW	$m_0 = 2112.3 \pm 0.5$, $\Gamma_0 = 1.9$
$D_{s0\,v}^*(2317)^-$	0	$m^2(\overline{D}^0K^-)$	RBW	$m_0 = 2317.8 \pm 0.6$, $\Gamma_0 = 3.8$
B_v^{*+}	1	$m^2(\overline{D}^0\pi^+)$	RBW	$m_0 = 5325.2 \pm 0.4$, $\Gamma_0 = 0$

Dalitz plot anlayses: $B^0 \to \bar{D}^0\pi^+\pi^-$ [PRD 92 (2015) 032002]

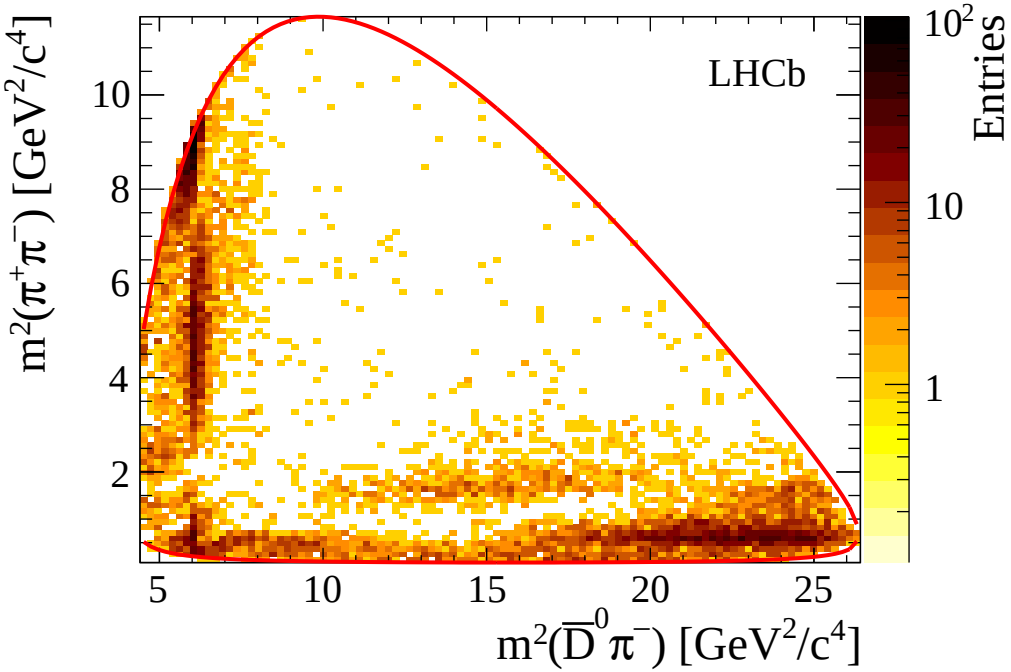

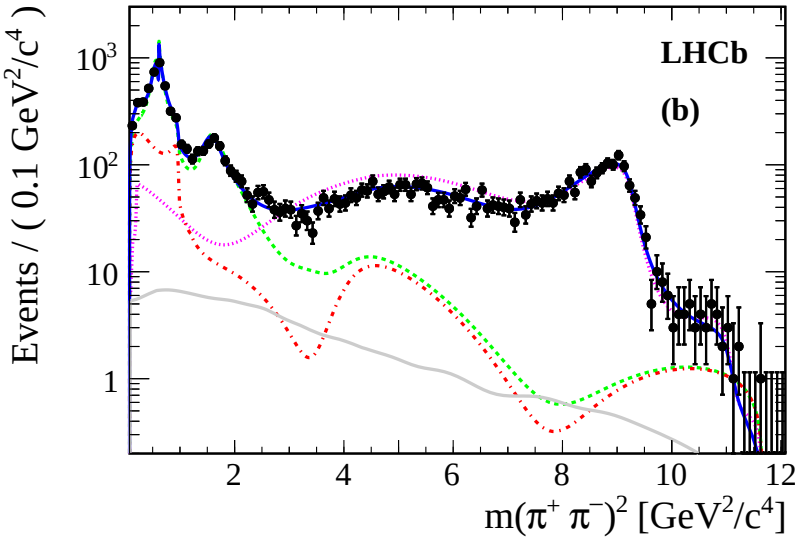

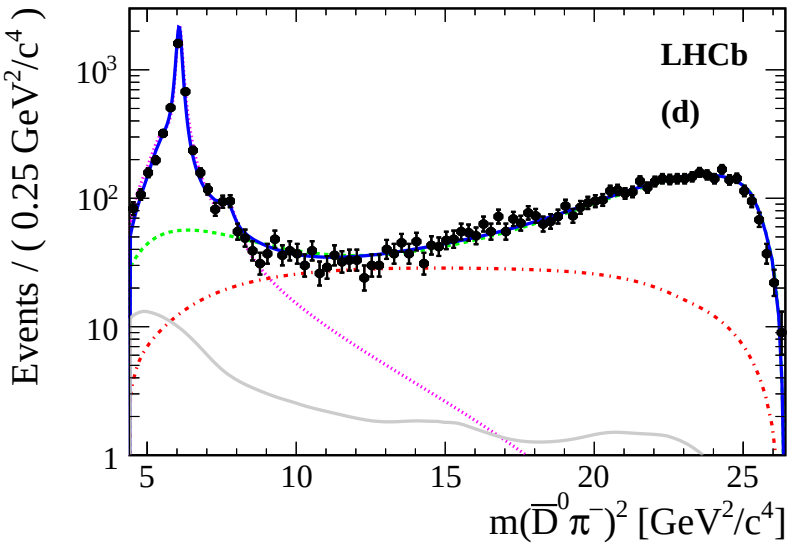

Resonance	Spin	Model	m_r (MeV/c^2)	Γ_0 (MeV)
$\bar{D}^0\pi^-$ P-wave	1	Eq. ??	Floated	
$D_0^*(2400)^-$	0	RBW	Floated	
$D_2^*(2460)^-$	2	RBW	Floated	
$D_J^*(2760)^-$	3	RBW	Floated	
$\rho(770)$	1	GS	775.02 ± 0.35	149.59 ± 0.67
$\omega(782)$	1	Eq. ??	781.91 ± 0.24	8.13 ± 0.45
$\rho(1450)$	1	GS	1493 ± 15	427 ± 31
$\rho(1700)$	1	GS	1861 ± 17	316 ± 26
$f_2(1270)$	2	RBW	1275.1 ± 1.2	$185.1 ^{+2.9}_{-2.4}$
$\pi\pi$ S-wave	0	K-matrix	See Sec. ??	
$f_0(500)$	0	Eq. ??	See Sec. ??	
$f_0(980)$	0	Eq. ??	See Sec. ??	
$f_0(2020)$	0	RBW	1992 ± 16	442 ± 60
Nonresonant	0	Eq. ??	See Sec. ??	

Dalitz plot anlayses: $B^0 \to \bar{D}^0\pi^+\pi^-$ [PRD 92 (2015) 032002]

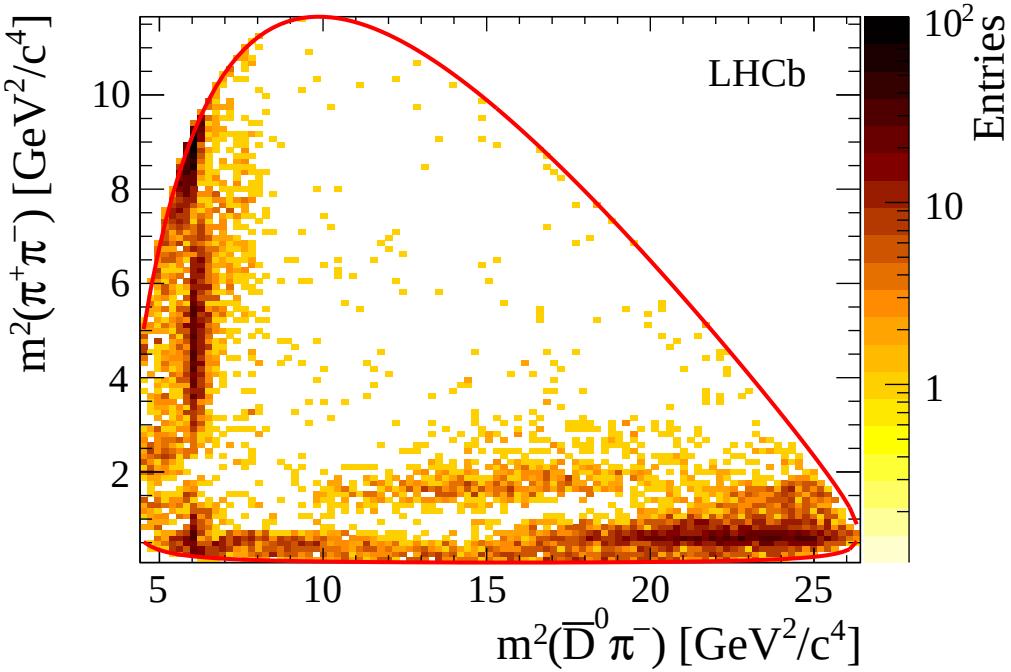

$D_J^*(2760)$:

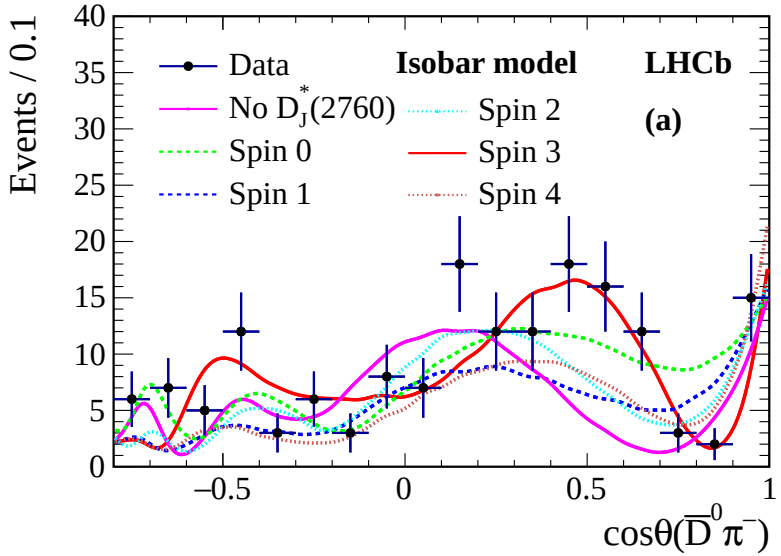

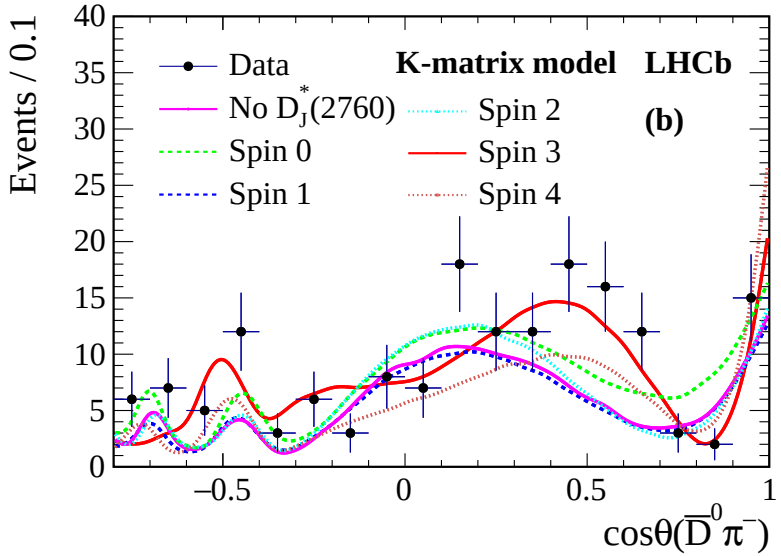

Resonance	Spin	Model	m_r (MeV/c^2)	Γ_0 (MeV)
$\bar{D}^0\pi^-$ P-wave	1	Eq. ??	Floated	
$D_0^*(2400)^-$	0	RBW	Floated	
$D_2^*(2460)^-$	2	RBW	Floated	
$D_J^*(2760)^-$	3	RBW	Floated	
$\rho(770)$	1	GS	775.02 ± 0.35	149.59 ± 0.67
$\omega(782)$	1	Eq. ??	781.91 ± 0.24	8.13 ± 0.45
$\rho(1450)$	1	GS	1493 ± 15	427 ± 31
$\rho(1700)$	1	GS	1861 ± 17	316 ± 26
$f_2(1270)$	2	RBW	1275.1 ± 1.2	$185.1 ^{+2.9}_{-2.4}$
$\pi\pi$ S-wave	0	K-matrix	See Sec. ??	
$f_0(500)$	0	Eq. ??	See Sec. ??	
$f_0(980)$	0	Eq. ??	See Sec. ??	
$f_0(2020)$	0	RBW	1992 ± 16	442 ± 60
Nonresonant	0	Eq. ??	See Sec. ??	

Comparison of isobar and K-matrix for spin-0 $\pi^+\pi^-$ wave

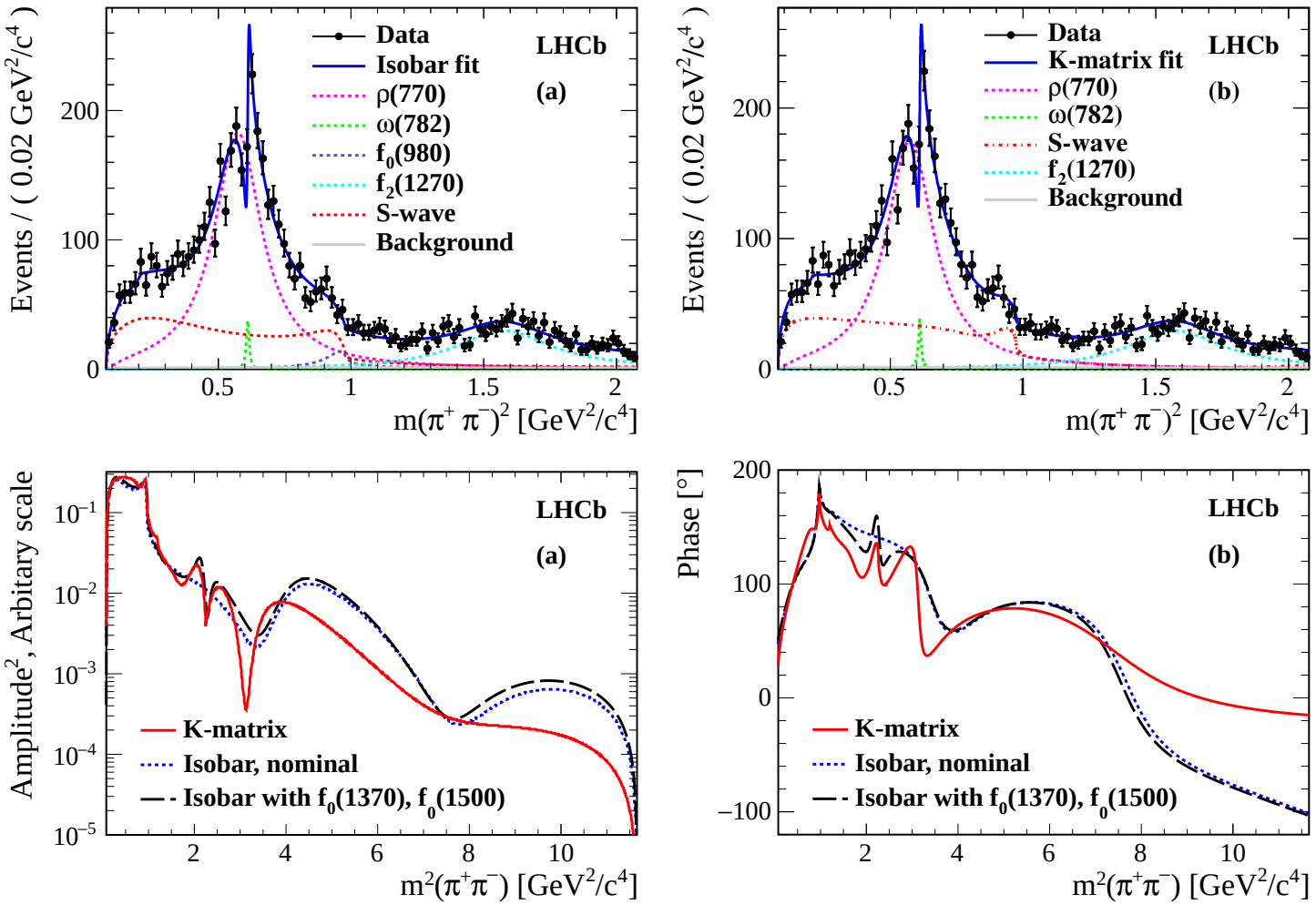

There are differences, but the effect on the fit quality is small.

Model-independent approaches: Legendre moments

Allow to investigate the helicity structure as a function of m^2 *without* performing a fit.
Use the fact that partial wave with spin J is a Legendre polynomial $P_J(\cos\theta_{\rm hel})$.

Weight events as functions of helicity:

$$w_i = P_L(\cos\theta_{\rm hel})$$

Partial waves with spins up to J give moments up to $2J$ in the event density.

If we are limited to S, P and D waves:

$$\begin{aligned}
\langle P_0\rangle &= |h_0|^2 + |h_1|^2 + |h_2|^2 \\
\langle P_1\rangle &= \frac{2}{\sqrt{3}}|h_0||h_1|\cos\delta_{01} + \frac{4}{\sqrt{15}}|h_1||h_2|\cos\delta_{12} \\
\langle P_2\rangle &= \frac{2}{\sqrt{5}}|h_0||h_2|\cos\delta_{02} + \frac{2}{5}|h_1|^2 + \frac{2}{7}|h_2|^2 \\
\langle P_3\rangle &= \frac{6}{7}\sqrt{\frac{3}{5}}|h_1||h_2|\cos\delta_{12} \\
\langle P_4\rangle &= \frac{2}{7}|h_2|^2
\end{aligned}$$

Legendre moments: $B^- \to D^+ K^- \pi^-$ [PRD 91 (2015) 092002]

Resonances only in one channel: $D^+\pi^-$: ideal for Legendre polynomial approach

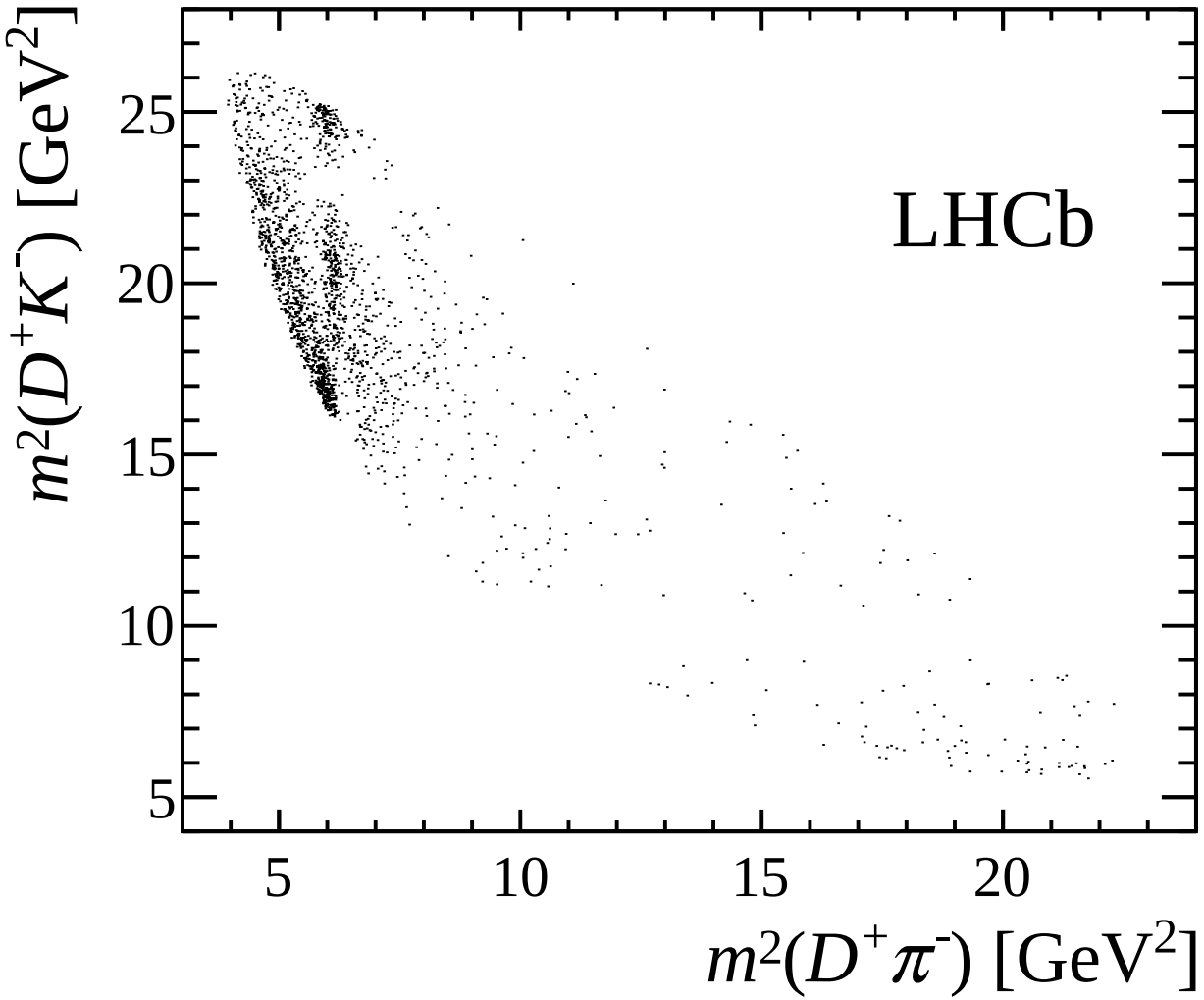

Consider contributions up to spin-3:

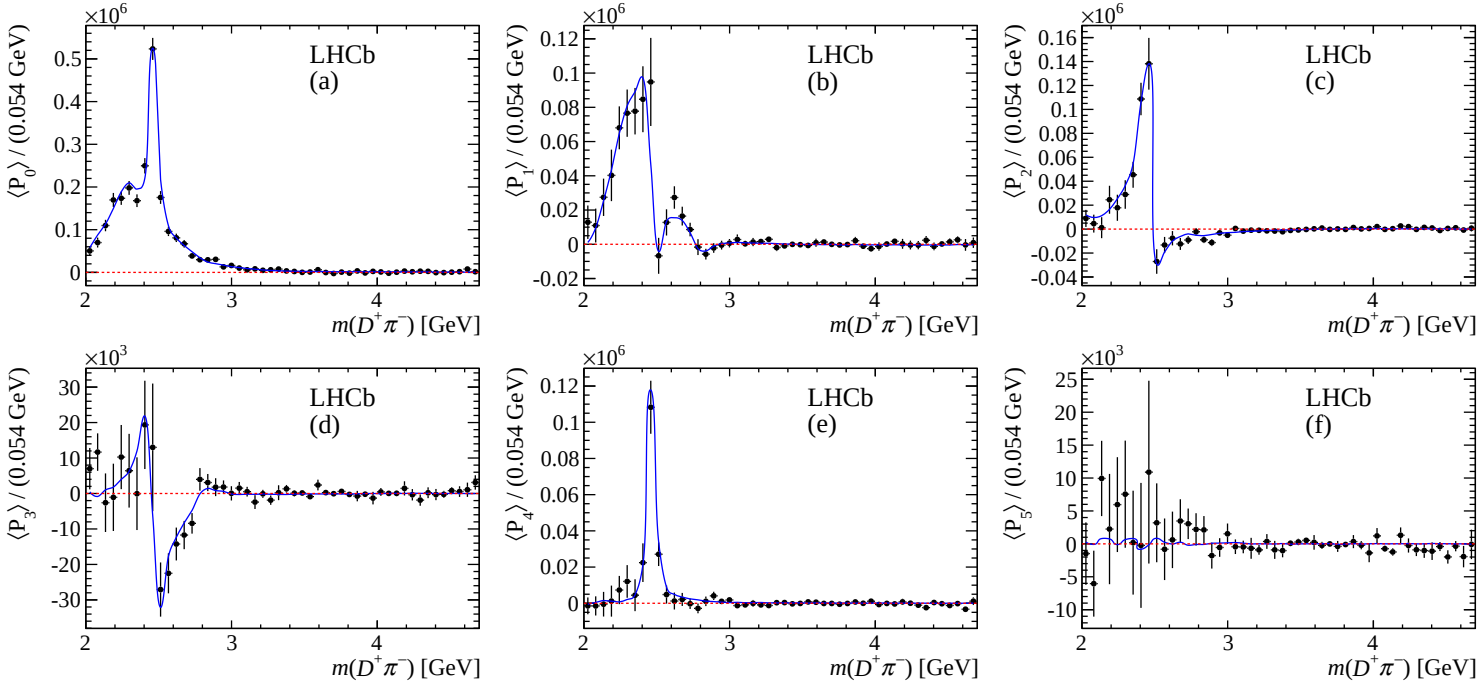

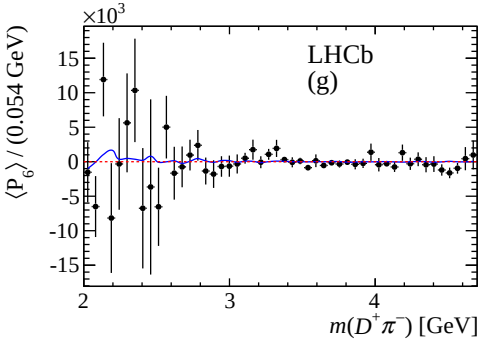

- Moments 6 and 7 consistent with 0: no evidence for PW with spin-3.
- Spin-2 apparent in moment 4: single state $D_2^*(2460)$
- Moment 3 differs from 4: interference with spin-2 and broad spin-1
- Moments 1 and 3 differ again: interference of spin-1 and spin-0 (broad as well)

Legendre moments: $B^- \to D^+\pi^-\pi^-$ [arXiv:1608.01289]

Resonances only in $D^+\pi^-$, but two identical pions in the final state: need to symmetrise the amplitude

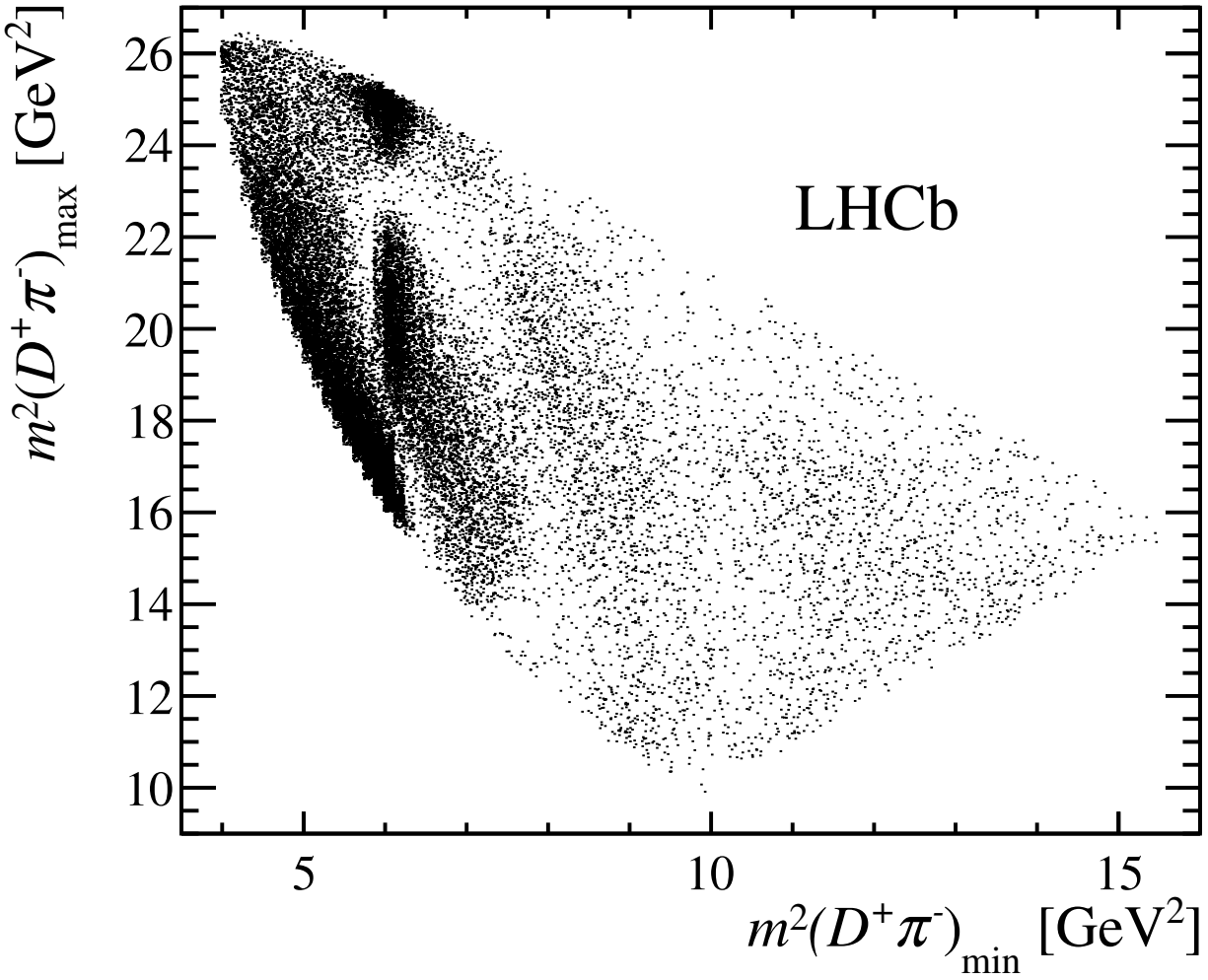

Legendre moments: $B^- \to D^+\pi^-\pi^-$ [arXiv:1608.01289]

Consider contributions up to spin-3:

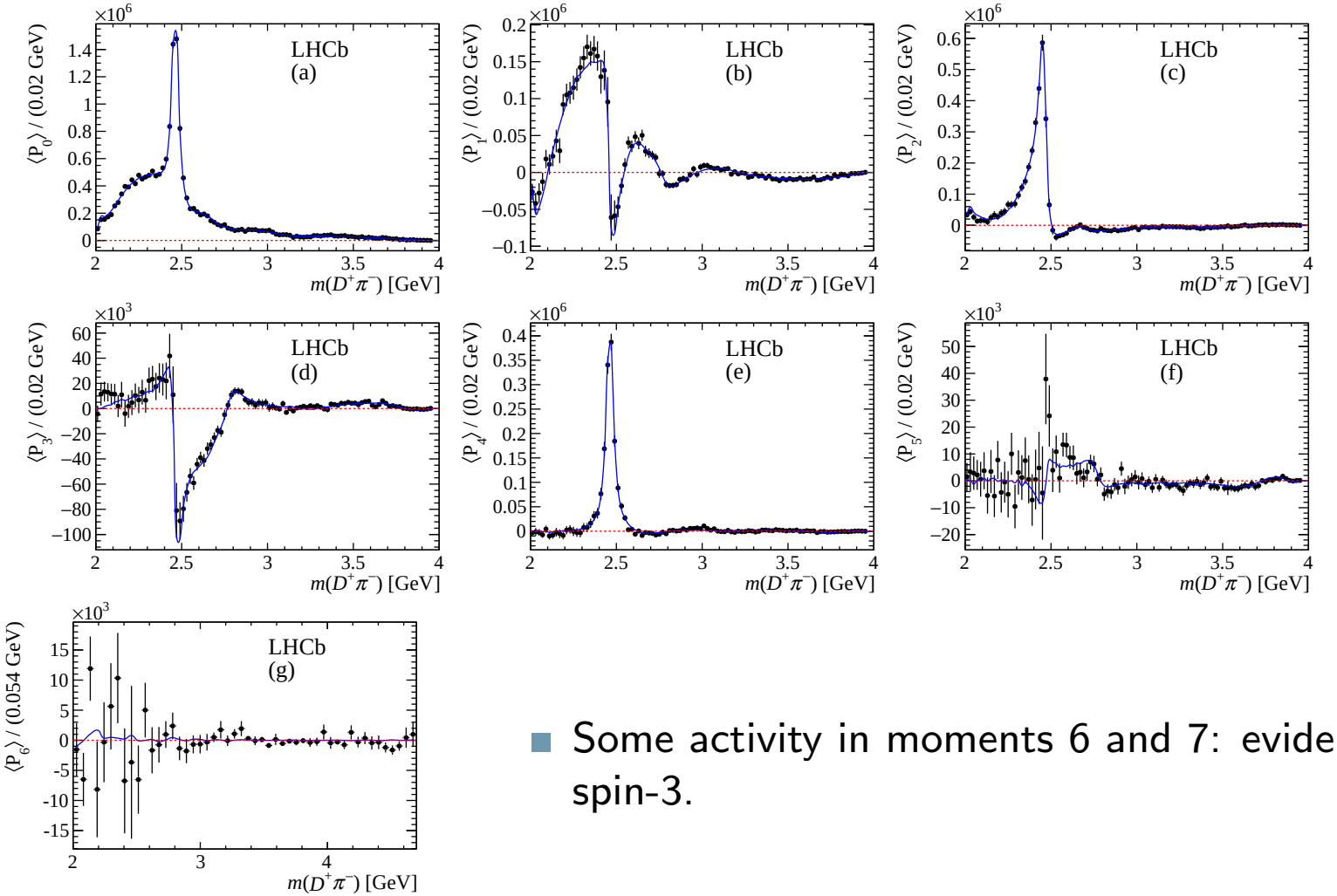

- Some activity in moments 6 and 7: evidence for PW with spin-3.

Model-independent S-wave: $B^- \to D^+\pi^-\pi^-$ [arXiv:1608.01289]

Large data sample allows to describe the S-wave by a model-independent spline-interpolated shape.
$Re(A)$ and $Im(A)$ in each node are fitted.
Interference with higher-spin waves provides information about the phase.

Resonance	Spin	Model	Parameters
$D_2^*(2460)^0$	2	RBW	Determined from data (see Table **??**)
$D_1^*(2680)^0$	1	RBW	
$D_3^*(2760)^0$	3	RBW	
$D_2^*(3000)^0$	2	RBW	
$D_v^*(2007)^0$	1	RBW	$m = 2006.98 \pm 0.15\,\text{MeV}$, $\Gamma = 2.1\,\text{MeV}$
B_v^{*0}	1	RBW	$m = 5325.2 \pm 0.4\,\text{MeV}$, $\Gamma = 0.0\,\text{MeV}$
Total S-wave	0	MIPW	See text

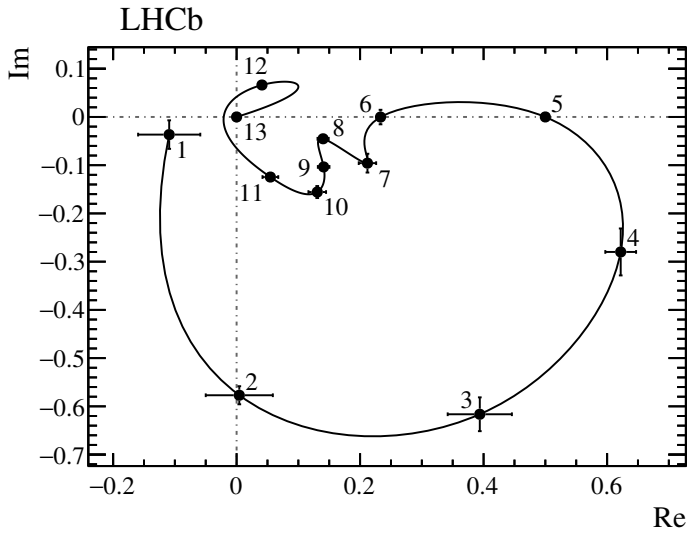

Phase rotation due to resonant $D^*(2400)$ state.

Non-scalars in the final state

Non-scalar particle in the final state adds more degrees of freedom to the 2D 3-body phase space

Examples:

- $B^0 \to \psi' \pi^- K^+$, $\psi' \to \mu^+\mu^-$: 4 variables in the phase space

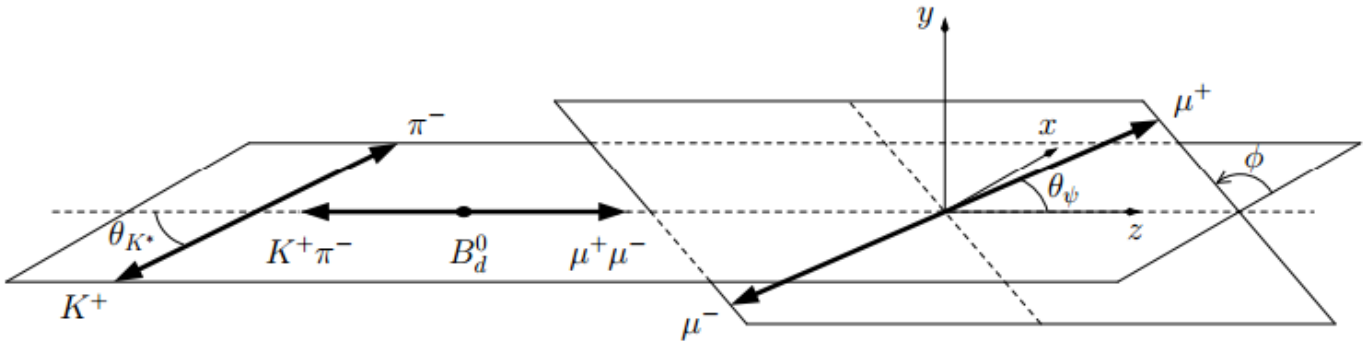

- $B^+ \to J/\psi\, \phi K^+$, $J/\psi \to \mu^+\mu^-$, $\phi \to K^+K^-$: 6 variables in the phase space

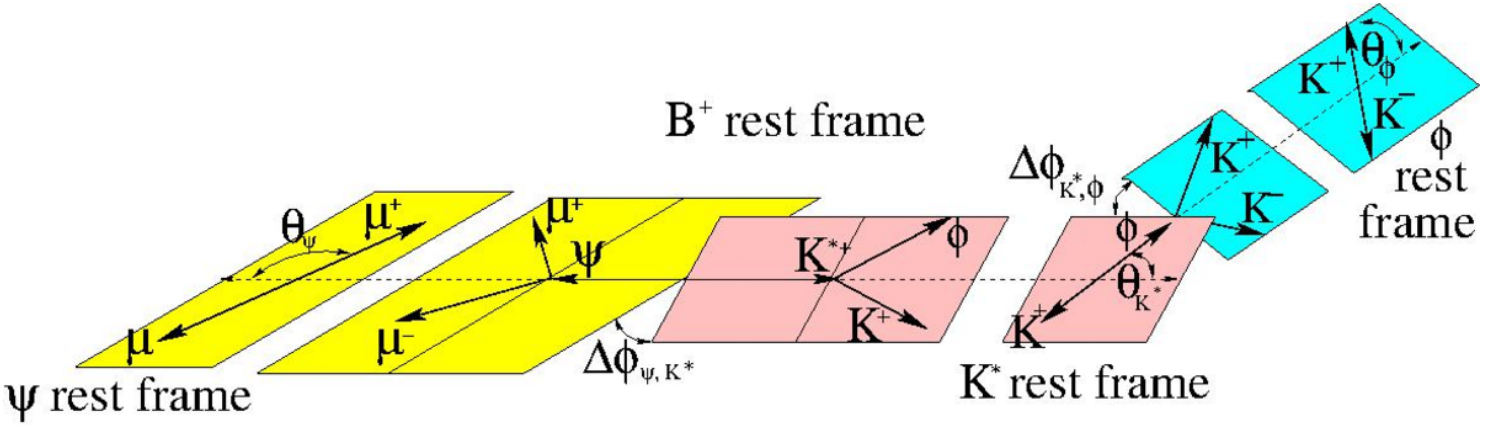

Non-scalars in the final state: helicity formalism

- Decay density is an incoherent sum of several spin configurations

$$P(\Omega) = \sum_{\Delta\lambda_\mu} \sum_{\lambda_{\Lambda_b^0}} \sum_{\lambda_p} |M_{\Delta\lambda_\mu, \lambda_{\Lambda_b^0}, \lambda_p}(\Omega)|^2$$

- Each resonant amplitude is factorised into quasi-tow-body $A \to BC$ helicity amplitudes

$$M^{A\to BC} = A_{\lambda_B, \lambda_C} D^{J_C}_{\lambda_A, \lambda_B - \lambda_C}(\phi, \theta, 0)$$

- Each resonance does not correspond to a unique amplitude. Several couplings for the same resonance:

$$A_{\lambda_B, \lambda_C} = \sum_L \sum_S \sqrt{\frac{2L+1}{2J_A+1}} B_{L,S} \left(\begin{array}{cc|c} J_B & J_C & S \\ \lambda_B & -\lambda_C & \lambda_B - \lambda_C \end{array} \right) \times \left(\begin{array}{cc|c} L & S & J_A \\ 0 & \lambda_B - \lambda_C & \lambda_B - \lambda_C \end{array} \right)$$

  Often convenient to reduce the number of couplings to the lowest possible L

- Bonus: ampltudes become sensitive to P parities of the resonances
- Angles for different decay chain are defined differently, but are not independent. Helicity states for different chains should be rotated to the same basis in coherent sum.

Non-scalars in the final state: $B^0 \to \psi' \pi^- K^+$ [PRL 112 (2014) 222002]

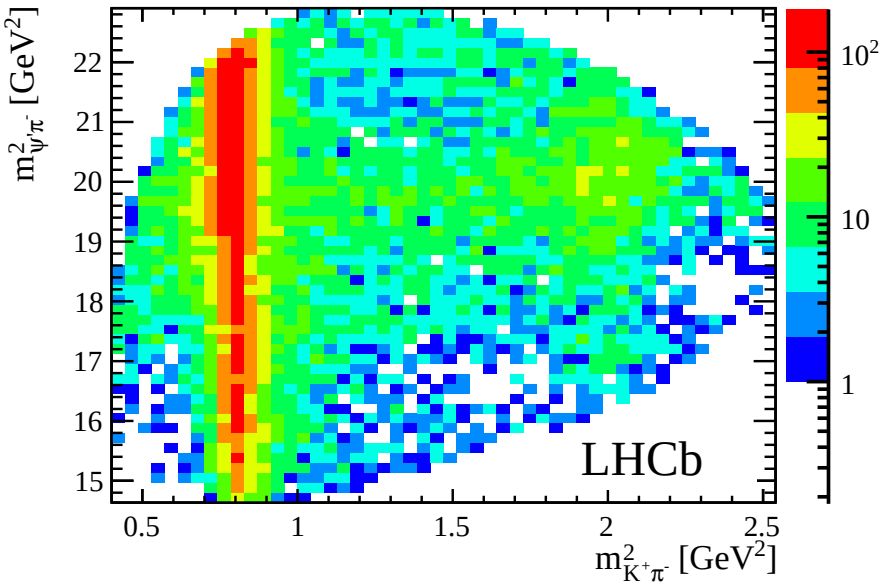

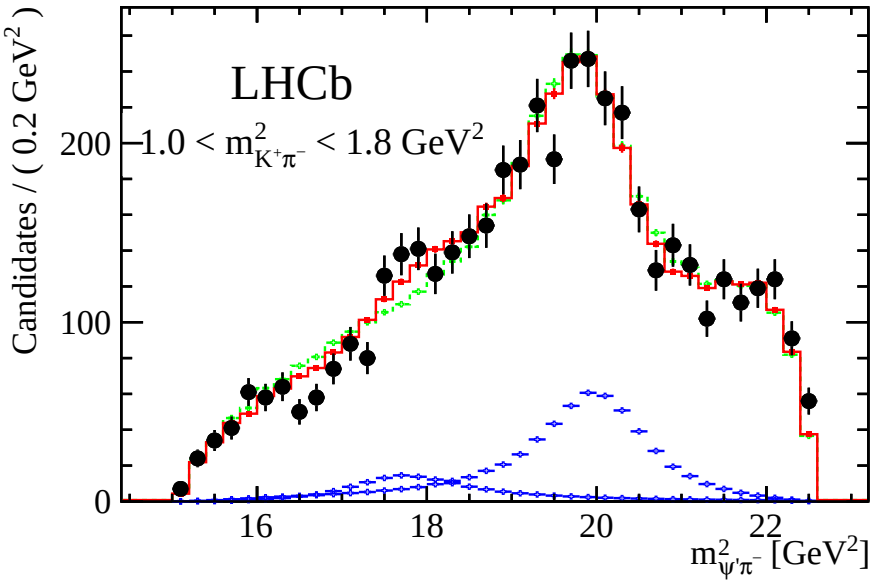

- K^* resonances: $K_0^*(800)$, $K^*(892)$, $K^*(1410)$, $K_{0,2}^*(1430)$, $K^*(1680)$
- Z states:
  - $J^P = 1^+$, 14σ:
    $M = 4475 \pm 7^{+15}_{-25}$ MeV/c^2,
    $\Gamma = 172 \pm 13^{+37}_{-34}$ MeV
  - $J^P = 0^-$, 6σ:
    $M = 4239 \pm 18^{+45}_{-10}$ MeV/c^2,
    $\Gamma = 220 \pm 47^{+108}_{-74}$ MeV

Non-scalars in the final state: $B^0 \to \psi' \pi^- K^+$ [PRL 112 (2014) 222002]

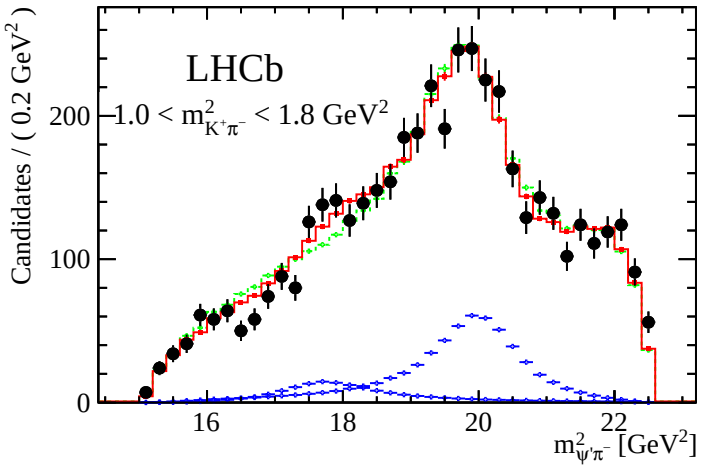

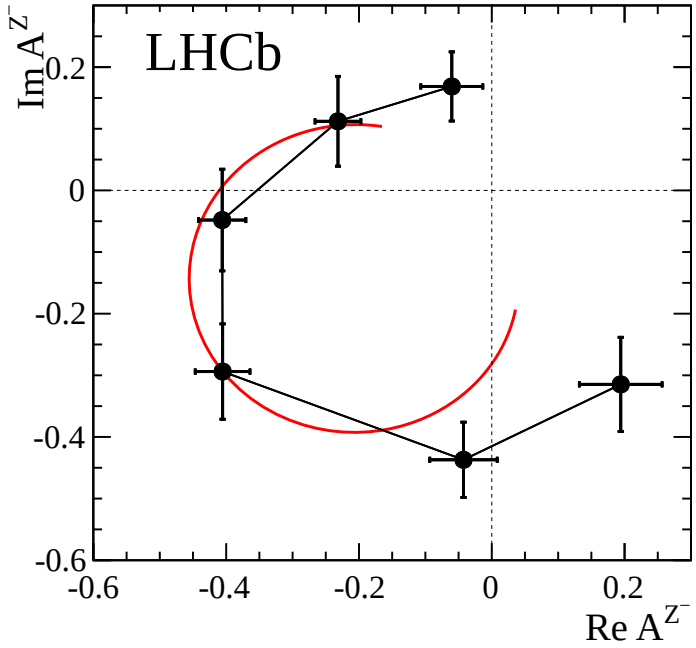

- Model-independent confirmation of phase rotation in $\psi' \pi^-$ amplitude: Argand plot with 6 bins in the range $18 < m^2(\psi' \pi^-) < 21.5\,\mathrm{GeV}/c^2$.
- $Re(A)$ and $Im(A)$ floated independently in each bin
- Interference with the $K^- \pi^+$ amplitude provides access to the phase

First 6 normalised Legendre moments

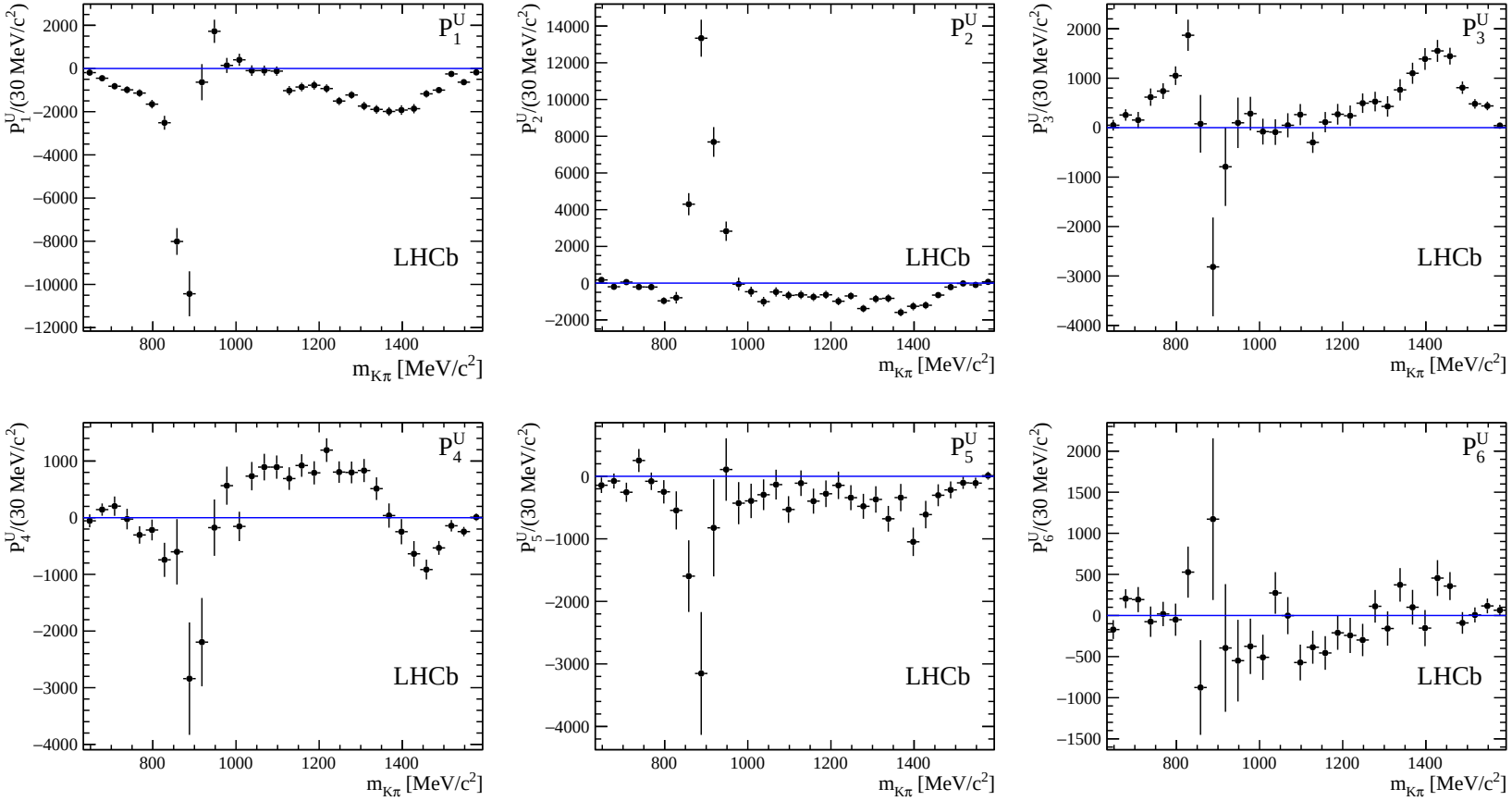

Model-independent approach: $B^0 \to \psi' \pi^- K^+$ [PRD 92 (2015) 112009]

Model-independent confirmation of the exotic contribution.
Check that $K^-\pi^+$ amplitude fails to describe the amplitude.
$K^-\pi^+$ should contribute to reasonably low moments, while exotic $\psi'\pi^-$ contributes to *all* moments.

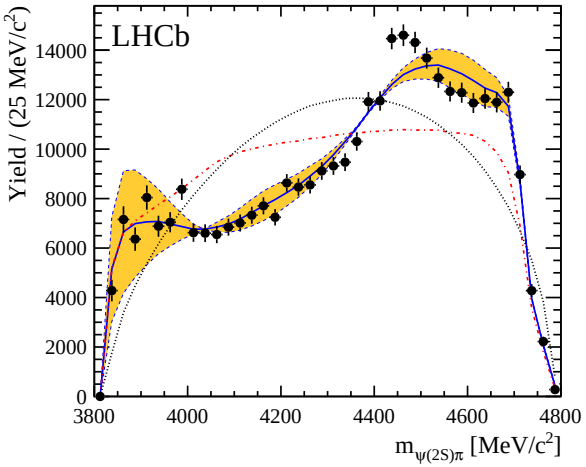

$l_{\max} = 4$

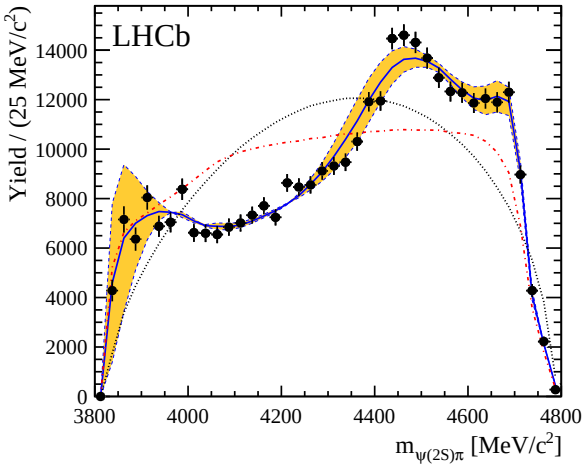

$l_{\max} = 6$

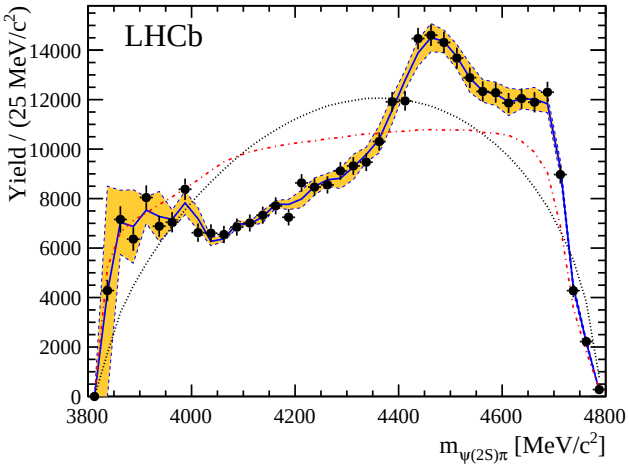

$l_{\max} = 30$

Test statistic:

$$-2\Delta NLL = -2 \sum_i \frac{W_i}{\epsilon_i} \log \frac{F_l(m^i_{\psi\pi})}{F_{30}(m^i_{\psi\pi})}$$

Run toys with $K^+\pi^-$-only model to determine distribution, compare with result in data.

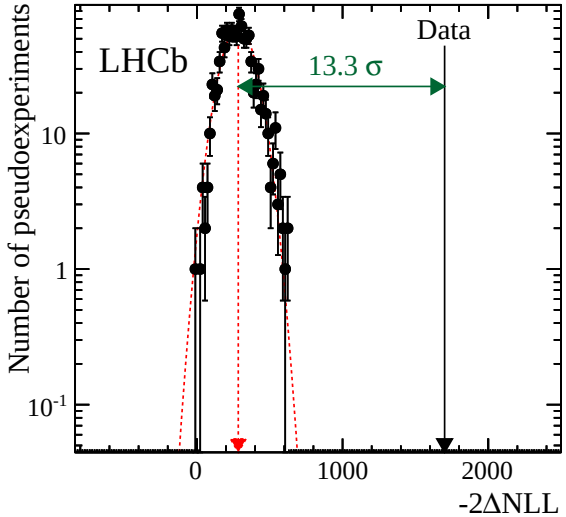

$l_{\max} = 4$

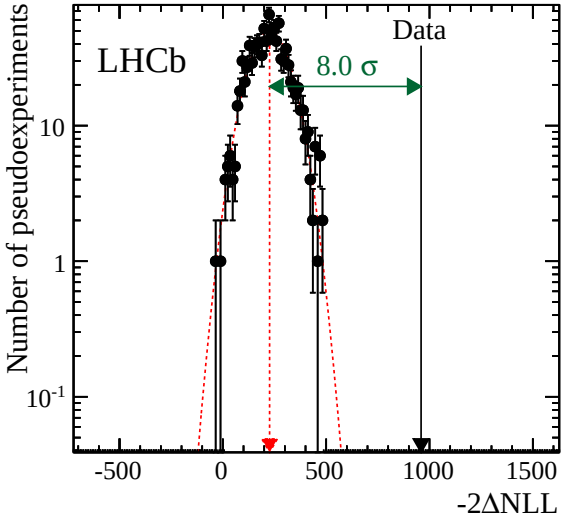

$l_{\max} = 6$

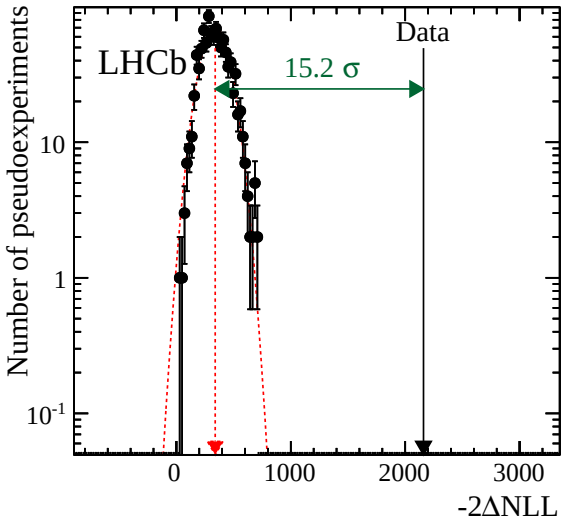

$l_{\max} = 4 \ldots 6$ depending on $m(K^+\pi^-)$

Non-scalars in the final state: $B^+ \to J/\psi\,\phi K^+$ [arXiv:1606.07898]

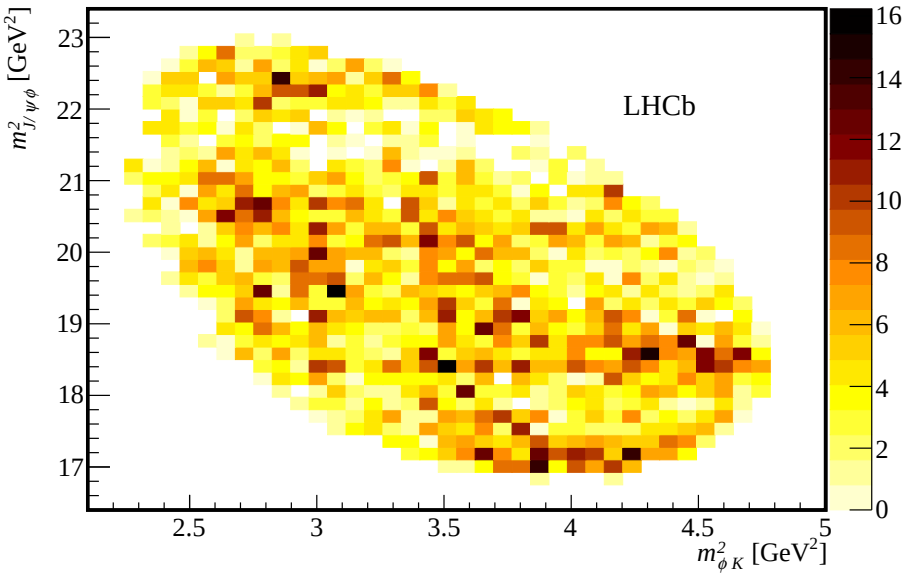

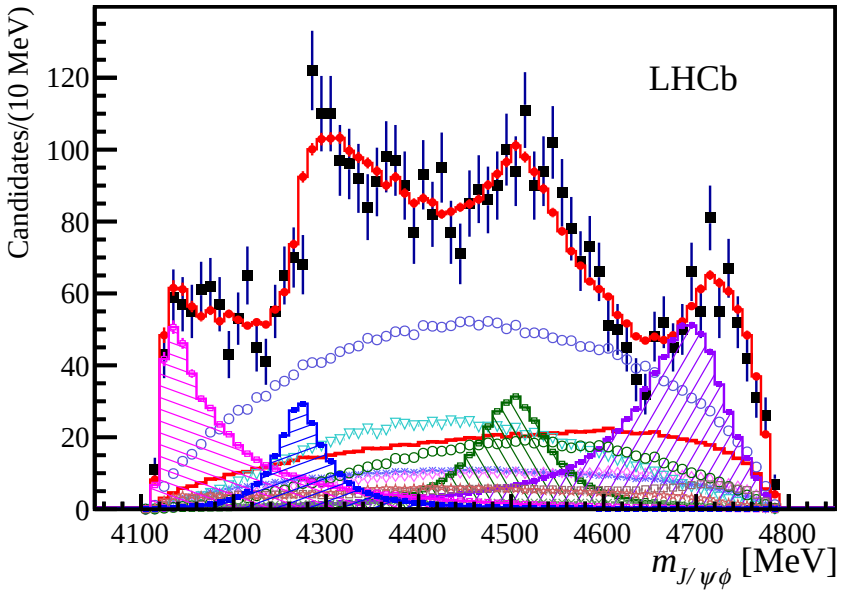

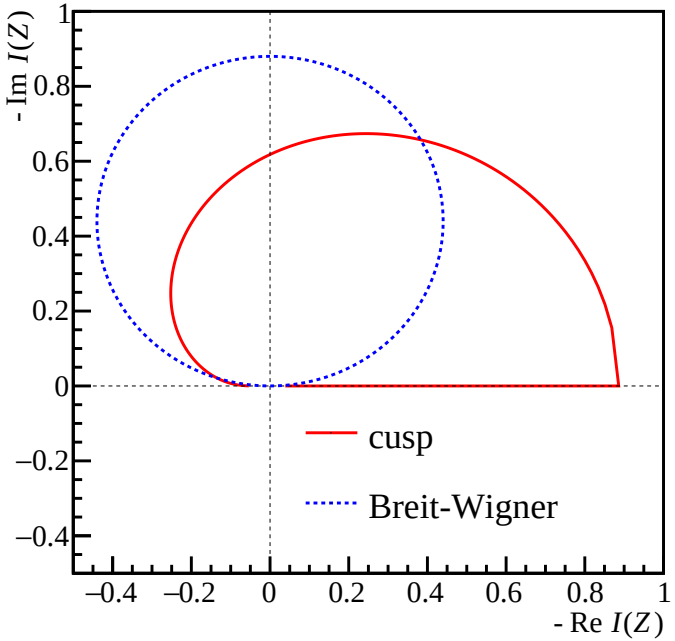

Statistics are not enough for model-independent lineashapes of X states.
More data should distinguish cusps and resonances

Amplitude analyses of baryons

Initial state is not a pure quantum state.

- In general: polarisation (dependent on production kinematics).
- Longitudinal polarisation violates parity, transverse still possible.
- In case of Λ_b^0: polarisation consistent with zero at LHCb.

$\Lambda_b^0 \to J/\psi\, pK^-$: 6D phase space for polarised Λ_b^0 ($M_{K^-\pi^+}$ and 5 helicity angles)

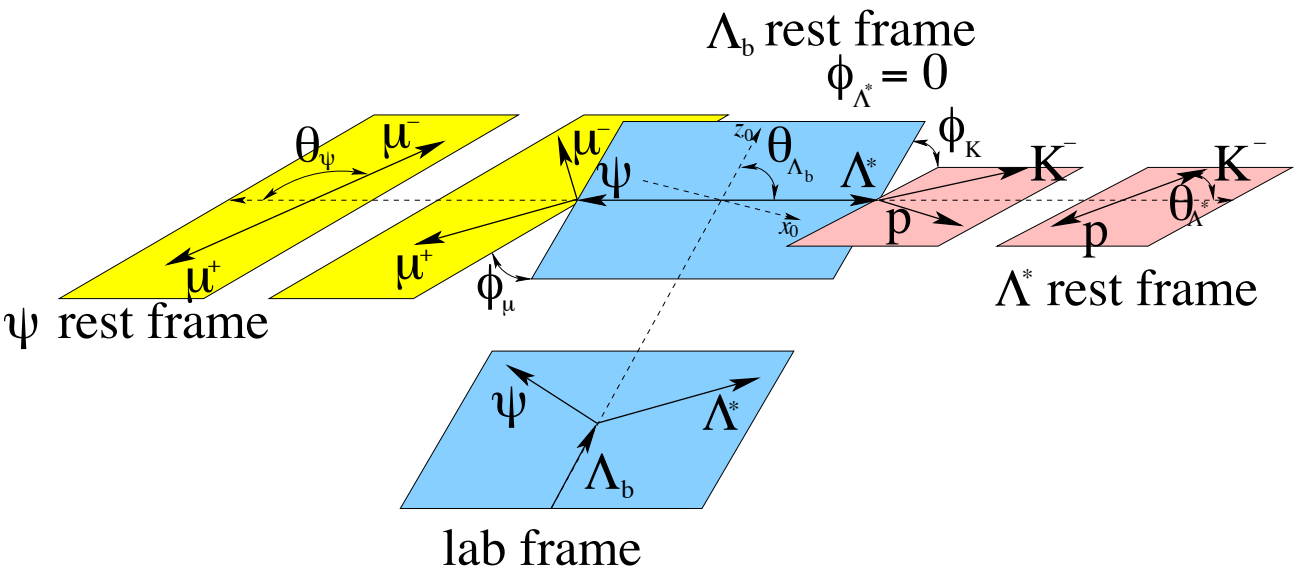

Amplitude analyses of baryons: $\Lambda_b^0 \to J/\psi\, pK^-$ [PRL 115 (2015) 072001]

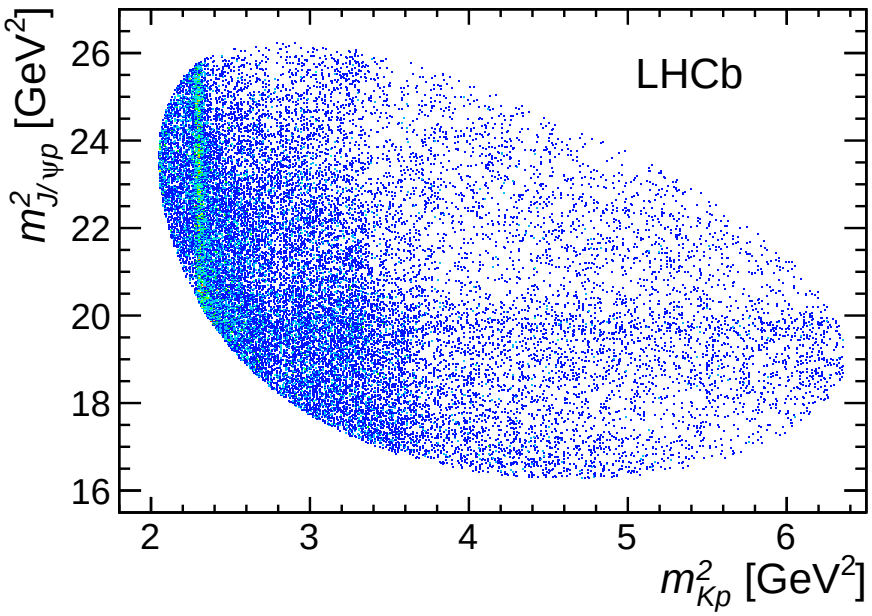

State	J^P	M_0 (MeV)	Γ_0 (MeV)	# Reduced	# Extended
$\Lambda(1405)$	$1/2^-$	$1405.1^{+1.3}_{-1.0}$	50.5 ± 2.0	3	4
$\Lambda(1520)$	$3/2^-$	1519.5 ± 1.0	15.6 ± 1.0	5	6
$\Lambda(1600)$	$1/2^+$	1600	150	3	4
$\Lambda(1670)$	$1/2^-$	1670	35	3	4
$\Lambda(1690)$	$3/2^-$	1690	60	5	6
$\Lambda(1800)$	$1/2^-$	1800	300	4	4
$\Lambda(1810)$	$1/2^+$	1810	150	3	4
$\Lambda(1820)$	$5/2^+$	1820	80	1	6
$\Lambda(1830)$	$5/2^-$	1830	95	1	6
$\Lambda(1890)$	$3/2^+$	1890	100	3	6
$\Lambda(2100)$	$7/2^-$	2100	200	1	6
$\Lambda(2110)$	$5/2^+$	2110	200	1	6
$\Lambda(2350)$	$9/2^+$	2350	150	0	6
$\Lambda(2585)$	?	$\approx$2585	200	0	6

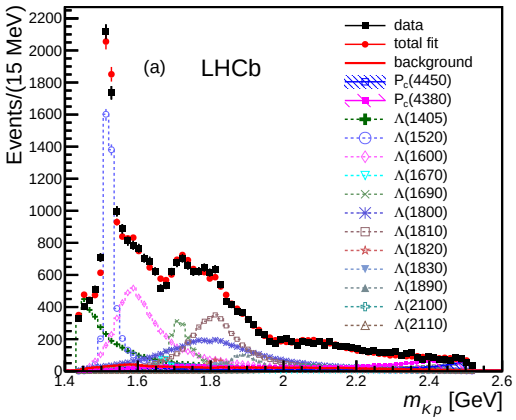

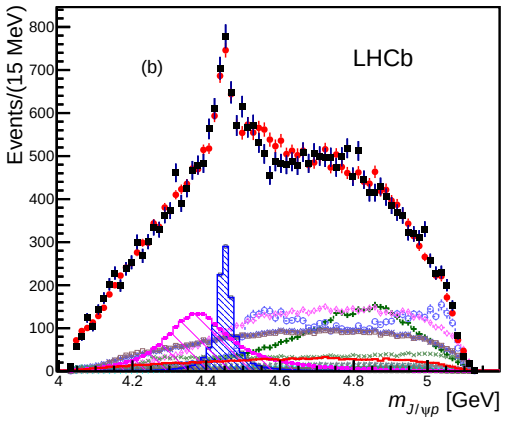

pK^- model: isobar with 12-14 Λ^* states from PDG.

Model-independent approach: $\Lambda_b^0 \to J/\psi\, pK^-$ [arXiv:1604.05708]

Checking that K^* resonances only cannot describe the data.
Use Legendre moments in $\cos\theta_{\rm hel}$ as a function of m_{pK}.
Allow $l_{\max}$ depending on m_{pK}

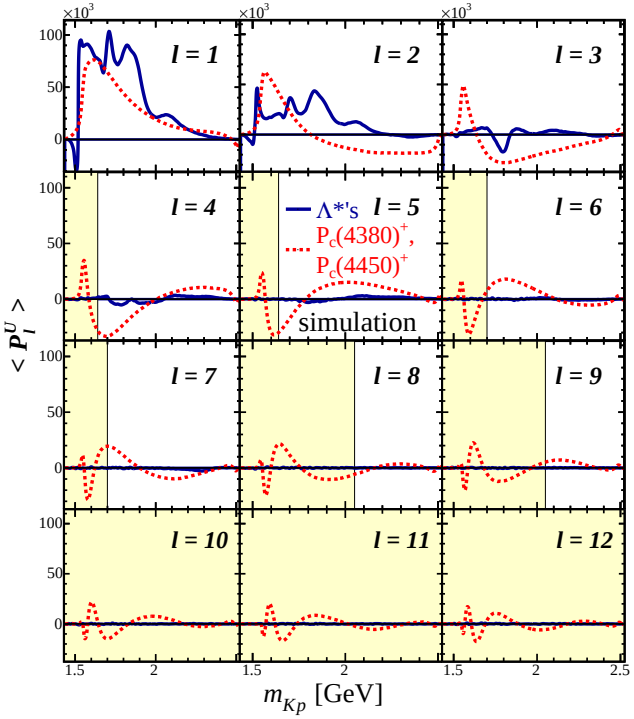

Moments from model

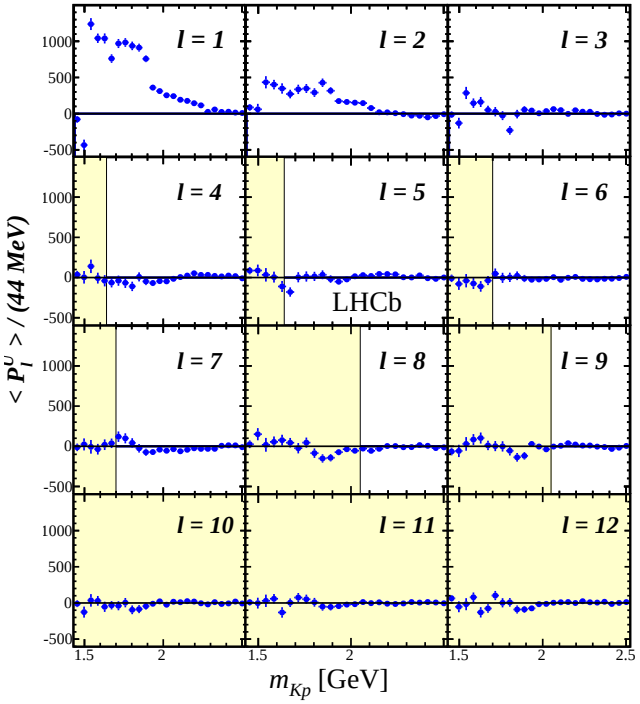

Moments from data

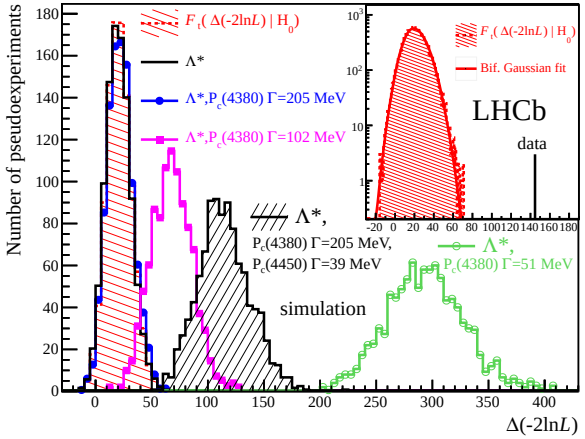

10σ significance

Amplitude analyses of baryons: $\Lambda_b^0 \to J/\psi\, p\pi^-$ [PRL 117 (2016) 082003]

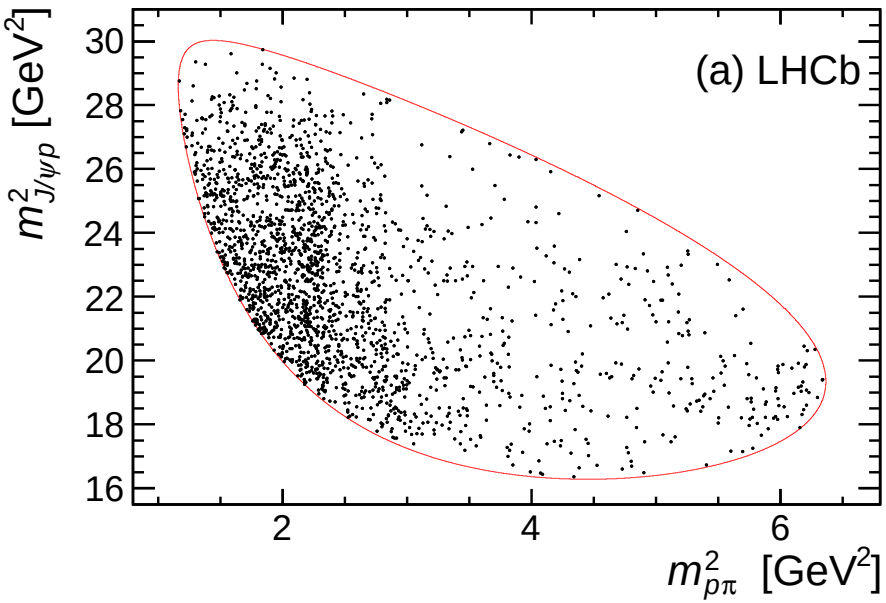

State	J^P	Mass (MeV)	Width (MeV)	RM	EM
NR $p\pi$	$1/2^-$	-	-	4	4
$N(1440)$	$1/2^+$	1430	350	3	4
$N(1520)$	$3/2^-$	1515	115	3	3
$N(1535)$	$1/2^-$	1535	150	4	4
$N(1650)$	$1/2^-$	1655	140	1	4
$N(1675)$	$5/2^-$	1675	150	3	5
$N(1680)$	$5/2^+$	1685	130	-	3
$N(1700)$	$3/2^-$	1700	150	-	3
$N(1710)$	$1/2^+$	1710	100	-	4
$N(1720)$	$3/2^+$	1720	250	3	5
$N(1875)$	$3/2^-$	1875	250	-	3
$N(1900)$	$3/2^+$	1900	200	-	3
$N(2190)$	$7/2^-$	2190	500	-	3
$N(2300)$	$1/2^+$	2300	340	-	3
$N(2570)$	$5/2^-$	2570	250	-	3
Free parameters				40	106

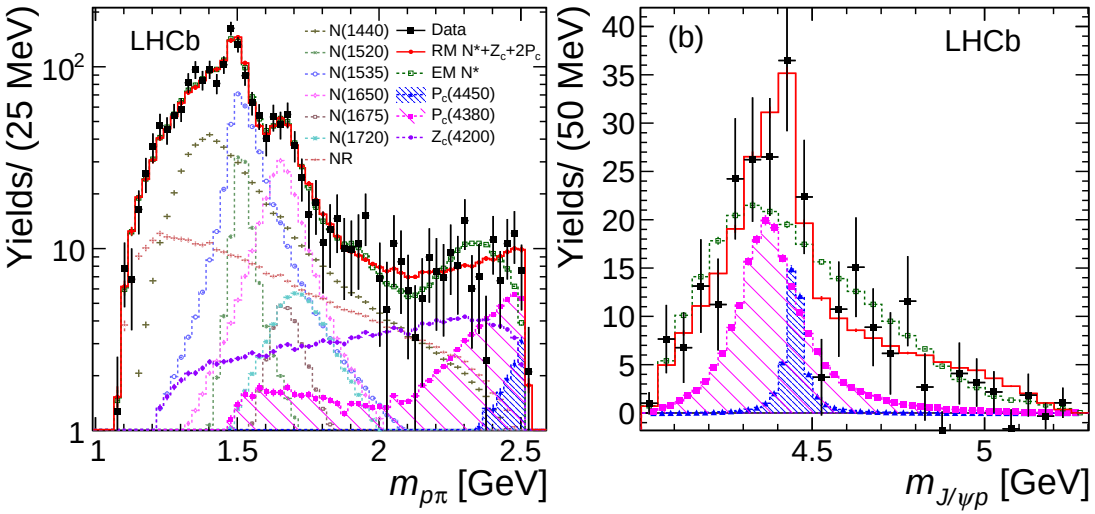

Basline: isobar $p\pi^-$ with 5-14 states.

Tried BW and Flatté for N(1535) (opening of $n\eta$ threshold)

Cross-check: K-matrix for $1/2^-$ using Bonn-Gatchina parametrisation

More constraints for $p\pi^-$ system: $\Lambda_b^0 \to D^0 p\pi^-$ [PRD 89 (2014) 032001]

Cabibbo-allowed contrary to $J/\psi\, p\pi^-$, twice as many events

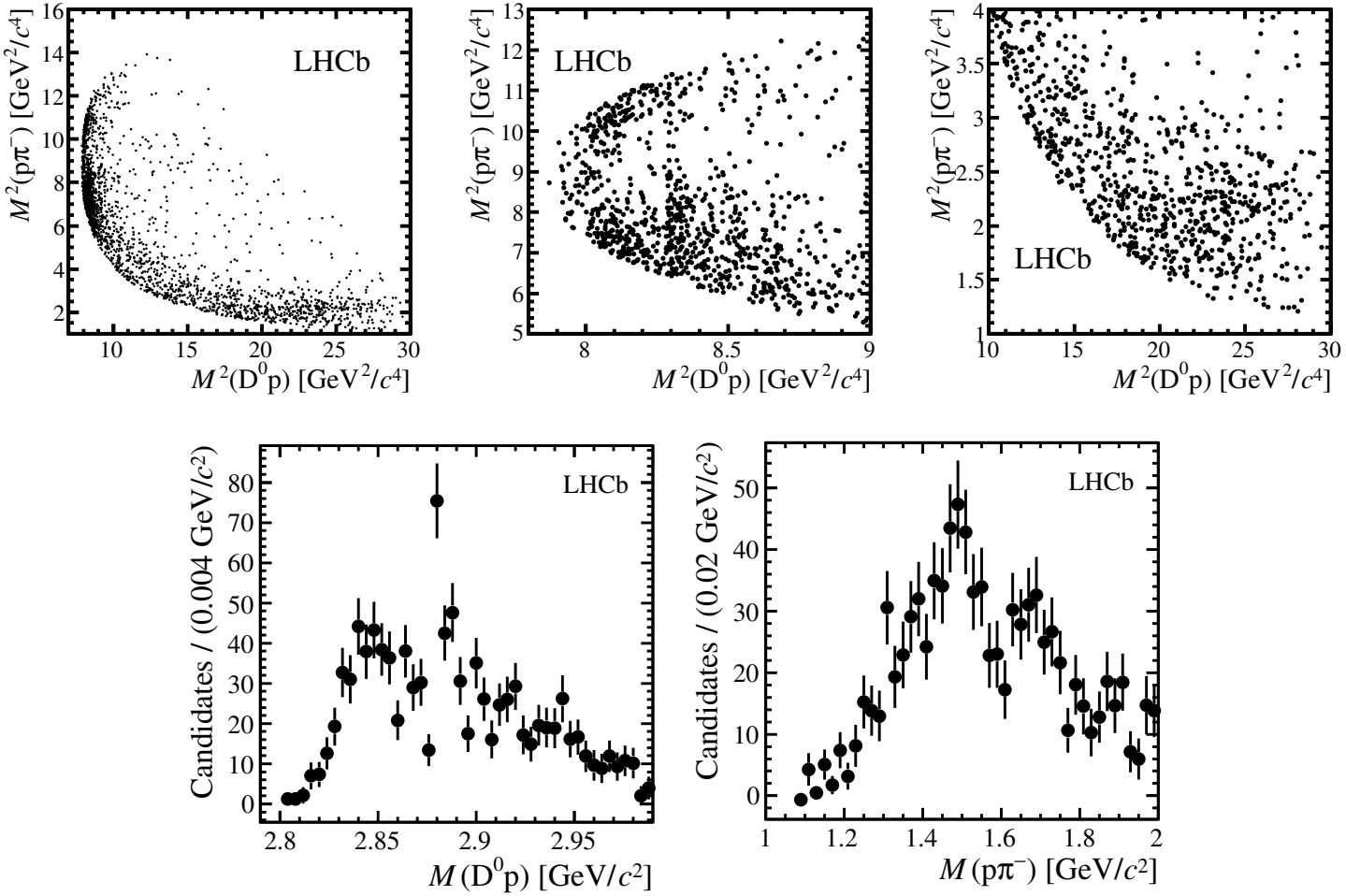

Plots from 1 fb^{-1} publication (no amplitude analysis), currently $\times 5$ as much data.
N^* as well as $\Lambda_c^* \to D^0 p$ states.

Conclusion

- Powerful analysis method gaining popularity at LHCb
  - Not only spectroscopy: NP searches ($B \to K\pi\pi\gamma$), CP violation ($B \to$charmless)
- Challenges ahead:
  - Multibody decays $\Rightarrow$ multidimensional phase space
  - Sophisticated amplitude models beyond isobar
  - Very large datasets
- Efficient tools and human expertise are needed

Multidimensional Resonance Analysis of $\Lambda_c^+ \to pK^-\pi^+$

E. M. Aitala,[i] S. Amato,[a] J. C. Anjos,[a] J. A. Appel,[e] D. Ashery,[n] S. Banerjee,[e] I. Bediaga,[a] G. Blaylock,[h] S. B. Bracker,[o] P. R. Burchat,[m] R. A. Burnstein,[f] T. Carter,[e] H. S. Carvalho,[a] N. K. Copty,[ℓ] L. M. Cremaldi,[i] C. Darling,[r] K. Denisenko,[e] S. Devmal,[c] A. Fernandez,[k] G. F. Fox,[ℓ] P. Gagnon,[b] C. Gobel,[a] K. Gounder,[i] A. M. Halling,[e] G. Herrera,[d] G. Hurvits,[n] C. James,[e] P. A. Kasper,[f] S. Kwan,[e] D. C. Langs,[ℓ] J. Leslie,[b] B. Lundberg,[e] J. Magnin,[a] S. MayTal-Beck,[n] B. Meadows,[c] J. R. T. de Mello Neto,[a] D. Mihalcea,[g] R. H. Milburn,[p] J. M. de Miranda,[a] A. Napier,[p] A. Nguyen,[g] A. B. d'Oliveira,[c,k] K. O'Shaughnessy,[b] K. C. Peng,[f] L. P. Perera,[c] M. V. Purohit,[ℓ] B. Quinn,[i] S. Radeztsky,[q] A. Rafatian,[i] N. W. Reay,[g] J. J. Reidy,[i] A. C. dos Reis,[a] H. A. Rubin,[f] D. A. Sanders,[i] A. K. S. Santha,[c] A. F. S. Santoro,[a] A. J. Schwartz,[c] M. Sheaff,[d,q] R. A. Sidwell,[g] A. J. Slaughter,[r] M. D. Sokoloff,[c] J. Solano,[a] N. R. Stanton,[g] R. J. Stefanski,[e] K. Stenson,[q] D. J. Summers,[i] S. Takach,[r] K. Thorne,[e] A. K. Tripathi,[g] S. Watanabe,[q] R. Weiss-Babai,[n] J. Wiener,[j] N. Witchey,[g] E. Wolin,[r] S. M. Yang,[g] D. Yi,[i] S. Yoshida,[g] R. Zaliznyak,[m] C. Zhang,[g]

Fermilab E791 Collaboration

[a] *Centro Brasileiro de Pesquisas Físicas, Rio de Janeiro RJ, Brazil*
[b] *University of California, Santa Cruz, California 95064*
[c] *University of Cincinnati, Cincinnati, Ohio 45221*
[d] *CINVESTAV, 07000 Mexico City, DF Mexico*
[e] *Fermilab, Batavia, Illinois 60510*
[f] *Illinois Institute of Technology, Chicago, Illinois 60616*
[g] *Kansas State University, Manhattan, Kansas 66506*

Preprint submitted to Elsevier Preprint 7 February 2008

CLNS 11/2082
CLEO 11-08

Amplitude analysis of $D^0 \to K^+K^-\pi^+\pi^-$

M. Artuso,[1] S. Blusk,[1] R. Mountain,[1] T. Skwarnicki,[1] S. Stone,[1] L. M. Zhang,[1] T. Gershon,[2] G. Bonvicini,[3] D. Cinabro,[3] A. Lincoln,[3] M. J. Smith,[3] P. Zhou,[3] J. Zhu,[3] P. Naik,[4] J. Rademacker,[4] D. M. Asner,[5,*] K. W. Edwards,[5] K. Randrianarivony,[5] G. Tatishvili,[5,*] R. A. Briere,[6] H. Vogel,[6] P. U. E. Onyisi,[7] J. L. Rosner,[7] J. P. Alexander,[8] D. G. Cassel,[8] S. Das,[8] R. Ehrlich,[8] L. Gibbons,[8] S. W. Gray,[8] D. L. Hartill,[8] B. K. Heltsley,[8] D. L. Kreinick,[8] V. E. Kuznetsov,[8] J. R. Patterson,[8] D. Peterson,[8] D. Riley,[8] A. Ryd,[8] A. J. Sadoff,[8] X. Shi,[8] W. M. Sun,[8] J. Yelton,[9] P. Rubin,[10] N. Lowrey,[11] S. Mehrabyan,[11] M. Selen,[11] J. Wiss,[11] J. Libby,[12] M. Kornicer,[13] R. E. Mitchell,[13] D. Besson,[14] T. K. Pedlar,[15] D. Cronin-Hennessy,[16] J. Hietala,[16] S. Dobbs,[17] Z. Metreveli,[17] K. K. Seth,[17] A. Tomaradze,[17] T. Xiao,[17] L. Martin,[18] A. Powell,[18] P. Spradlin,[18] G. Wilkinson,[18] J. Y. Ge,[19] D. H. Miller,[19] I. P. J. Shipsey,[19] B. Xin,[19] G. S. Adams,[20] J. Napolitano,[20] K. M. Ecklund,[21] J. Insler,[22] H. Muramatsu,[22] C. S. Park,[22] L. J. Pearson,[22] E. H. Thorndike,[22] S. Ricciardi,[23] and C. Thomas[18,23]

(CLEO Collaboration)

[1] *Syracuse University, Syracuse, New York 13244, USA*
[2] *University of Warwick, Coventry CV4 7AL, United Kingdom*
[3] *Wayne State University, Detroit, Michigan 48202, USA*
[4] *University of Bristol, Bristol BS8 1TL, United Kingdom*
[5] *Carleton University, Ottawa, Ontario, Canada K1S 5B6*
[6] *Carnegie Mellon University, Pittsburgh, Pennsylvania 15213, USA*
[7] *University of Chicago, Chicago, Illinois 60637, USA*
[8] *Cornell University, Ithaca, New York 14853, USA*
[9] *University of Florida, Gainesville, Florida 32611, USA*
[10] *George Mason University, Fairfax, Virginia 22030, USA*
[11] *University of Illinois, Urbana-Champaign, Illinois 61801, USA*
[12] *Indian Institute of Technology Madras, Chennai, Tamil Nadu 600036, India*
[13] *Indiana University, Bloomington, Indiana 47405, USA*
[14] *University of Kansas, Lawrence, Kansas 66045, USA*
[15] *Luther College, Decorah, Iowa 52101, USA*
[16] *University of Minnesota, Minneapolis, Minnesota 55455, USA*
[17] *Northwestern University, Evanston, Illinois 60208, USA*
[18] *University of Oxford, Oxford OX1 3RH, United Kingdom*
[19] *Purdue University, West Lafayette, Indiana 47907, USA*
[20] *Rensselaer Polytechnic Institute, Troy, New York 12180, USA*
[21] *Rice University, Houston, Texas 77005, USA*
[22] *University of Rochester, Rochester, New York 14627, USA*
[23] *STFC Rutherford Appleton Laboratory, Chilton, Didcot, Oxfordshire, OX11 0QX, United Kingdom*

(Dated: January 27, 2012)